TRUNCATIONS OF THE RESPONSE REGULATOR AGRA INHIBIT *STAPHYLOCOCCUS AUREUS* QUORUM SENSING

TRUNCATIONS OF THE RESPONSE REGULATOR AGRA INHIBIT *STAPHYLOCOCCUS AUREUS* QUORUM SENSING

By ALEXANDRA LAUREN RUYTER, H.BSc

A Thesis Submitted to the School of Graduate Studies in Partial Fulfillment of the Requirements for the Degree Master's of Science

DESCRIPTIVE NOTE

Master's of Science (2013) McMaster University (Medical Sciences) Hamilton, Ontario

TITLE: Truncations of the Response Regulator AgrA Inhibit *Staphylococcus aureus* Quorum Sensing

AUTHOR: Alexandra L. Ruyter, H.Bsc (Molecular Biology – McMaster University)

SUPERVISOR: Dr. James B. Mahony

NUMBER OF PAGES

To Mom & Dad
With all my love

ABSTRACT

Virulence in *Staphylococcus aureus* is largely mediated by the *accessory gene regulator* (agr) quorum sensing system. This regulatory system is activated by a secreted thiolactone peptide termed autoinducing peptide (AIP) and its receptor histidine kinase, AgrC. Interaction of extracellular AIP with a cognate AgrC receptor generates an intracellular signal that is transduced by conformational changes and phosphorylation events in a two-component sensor histidine kinase system. At the heart of the *agr* quorum-sensing cascade lies the two-component sensor histidine kinase, AgrC, and the response regulator protein, AgrA. Interaction of AgrC and AgrA, and the resulting phosphotransfer event results in expression from the divergent promoters P2 and P3, inducing expression of the master quorum-sensing regulator RNAIII and upregulating the *agr* operon respectively. Signal transduction systems function as intracellular information-processing pathways that link sensation of external stimuli to specific adaptive processes. In *S. aureus* in particular, these include the up-regulation of virulence factors and hemolysis production, biofilm formation, and colonization-based regulation of surface proteins and adhesion factors. As such, the interactions of these systems have become key targets in the design of small inhibitor compounds.

Through the creation of a protein truncation series, we proposed the development of a small protein for the inhibition of key protein-protein interactions involved in *S. aureus agr* two-component signaling. Herein, we demonstrate the efficacy of these protein truncations as dominant negative inhibitors of AgrC:AgrA interactions, likely acting as a dominant phosphoacceptor in place of endogenous AgrA. We provide

evidence of this function through *in vitro* hemolysis assays and phosphate-detection based gel electrophoresis.

With treatment of *S. aureus* infections, even those displaying antibiotic resistance, currently limited to combinatorial antibiotic treatments or surgical procedures, novel non-antibiotic therapeutic options are desperately needed and will be imperative for the maintenance and control of *S. aureus* infections in clinical and community settings.

ACKNOWLEDGEMENTS

The past two years have been filled with new experiences, new friends, and in incredible new knowledge base. First and foremost, I would to thank my Dr. James Mahony for allowing me to start journey under his supervision. Dr. Mahony has been a constant source of support, mentorship, and inspiration for this project. He continually taught me to push my scientific boundaries, generate novel ways to solve problems, and that small failures can lead to large successes. I am a better student and scientist as a result of his invaluable guidance. I would also like to thank my committee members Dr. Marie Elliot and Dr. Dawn Bowdish for their support, assistance, and belief in this thesis. They have been incredible resources throughout this journey, and without their positive influences and pushes for critical thinking, the outcome of this project would likely not be the same.

In the three years I have spent in the Mahony laboratory, from my undergraduate thesis to my Masters thesis, I have had the immense pleasure of meeting an absolutely incredible group of individuals. All of you have made this experience irreplaceable, and your assistance, support and friendship means the world to me. Dr. Christopher Stone, thank you for providing me with the skills and training to become a successful member of this laboratory, and doing so with patience and understanding. Your guidance and critical consideration of experimental design and results have helped to form my ideas into a competent thesis. Thank you for all of your assistance, and the laughs along the way. To David Bulir, thank you for being a sounding board of ideas, a generator of conversation and critical thinking, and comic relief on those days when things get stressful. Your

assistance has been invaluable, and I appreciate all that you have taught me. Ken Mwawasi, one of the most adept scientists I know, thank you for your help and guidance along this journey. The brainstorming sessions, protocol assistance and motivation is greatly appreciated. To Dan Waltho, Tiffany Leighton, Robert Clayden, Andrea Granados and Sylvia Chong, I cannot thank you enough for your friendship, support and assistance and hope all the best for your future endeavors. Finally, to Jodi Gilchrist, thank you a thousand times over for your friendship, support, and all the laughs along the way. I would not have come this far in this thesis project if it were not for you, and our conversations.

My parents have been a constant source of love and support, even in the face of insurmountable obstacles. They have never doubted or questioned my paths in life, only offered their wisdom, guidance and motivation. Without their continuous encouragement, inspiration, and never give up attitude I could not have come this far. Thank you to the moon and back, I am who I am because of you. To my birthmom, Leslie, you are an integral part of who I am, thank you for everything you have done in my life. Finally, to my boyfriend Steve, who has been on this journey with me from start to finish. You have graciously come along on this rollercoaster, and been there for me unfailingly during both the highs and the lows. Your support, cheerleading, and love have seen me through every step of this process, thank you.

TABLE OF CONTENTS

LIST OF TABLES

TABLE OF FIGURES

LIST OF ABBREVATIONS & SYMBOLS

ATP	Adenosine Triphosphate
agr	Accessory Gene Regulator
AHL	Acyl-Homoserine Lactone
AIP	Autoinducing Peptides
BLAST	Basic Local Alignment Search Tool
B-ME	β-mercaptoethanol
CA	C-terminal Catalytic and ATP-Binding
CA-MRSA	Community Associated MRSA
ccr	Cassette Chromosome Recobinases
cDNA	Complementary DNA
Ct	Threshold Cycle
DHp	Dimerization and Histidine Phosphotransfer Domain
DNA	Deoxyribonucelic Acid
ECL	Enhanced Chemiluminescence
EDTA	Ethylenediaminetetraacetic Acid
Erm	Erythormycin
GST	Glutathione-S-Transferase
HA-MRSA	Hospital Acquired MRSA
HF	High Fidelity
His_6	Common epitope tag composed of six sequential Histidine residues
HIV	Humane Immunodeficiency Virus
HK	Histidine Kinase
IPTG	Isopropyl- -Thiogalactopyranoside
Kan	Kanamycin
LB	Luria-Bertani Broth
LDAO	Lauryldimethylamine-oxide
MBP	Maltose Binding Protein
MCS	Multiple Cloning Site
MGE	Mobile Genetic Element
MRSA	Methicillin Resistant *Staphylococcus aureus*
MSCRAMM	Microbial Surface Components Recognizing Adhesive Matrix Molecules
NLS	Nuclear Localization Signal
OD	Optical Density
Ω	Ohms
PAGE	Polyacrylamide Gel Electrophoresis
PBS	Phosphate Buffered Saline
PBP	Penicillin Binding Protein
PCR	Polymerase Chain Reaction
qRT-PCR	Quantitative Real-Time Polymerase Chain Reaction
QS	Quorum Sensing

RNA	Ribonucleic Acid
REC	Regulatory Receiver Domain
RT	Reverse Transcription
SBA	Sheep's Blood Agar
SCC*mec*	Staphylococcal Cassette Chromosome *mec*
SCV	Small-Colony Variants
SDS	Sodium Dodecyl Sulfate
SOC	Super Optimal Broth with Catabolite Repression
SSTI	Skin and Soft Tissue Infection
TEMED	Tetramethlethylenediamine
TSA	Tryptic Soy Agar
TSB	Tryptic Soy Broth
TCSK	Two-Component Sensor Kinase
VISA	Vancomycin Intermediate *Staphylococcus aureus*
VRSA	Vancomycin Resistant *Staphylococcus aureus*

CHAPTER ONE

1.0 INTRODUCTION

1.1 The genera *Staphylococcus*

Members of the genus *Staphylococcus*, of the *Micrococcaceae* family, comprise 30 different taxa of Gram-positive, facultatively anaerobic, coagulase positive bacteria (Götz *et.al.*, 2006; Slonczewski *et.al.*, 2009). Members of this genus form cocci (0.5-0.15 µm in diameter) singularly, in pairs, tetrads, short chains, and irregular grape-like clusters. They are nonmotile, non-spore forming, and exhibit limited encapsulation. Staphylococci have broad environmental niches, and are predominate colonizers of skin, skin glands and the mucous membranes of humans, mammals and birds. Moreover, this pathogen can be isolated from soil, sand sources, seawater, fresh water, plant surfaces, feeds, food products including meat and dairy, on furniture, clothing, paper currency, dust and in the air (Götz *et.al.*, 2006). The coagulase positive species of Staphylococcus, including *Staphylococcus aureus*, can be considered significant pathogens with staphylococcal diseases including impetigo, toxic shock syndrome, skin and soft tissue infections, endocarditis, food poisoning, and cervisitis (Götz *et.al.*, 2006; Prax *et.al.*, 2013). To date, 70 species and several subspecies are classified within the genus *Staphylococcus* including *Staphylococcus aureus, Staphylococcus epidermidis, Staphylococcus caprae, and Staphylococcus pasteuri* (Prax *et.al.*, 2013).

1.1.1 Staphylococcal taxonomy

Staphylococcus, introduced in 1883 by Ogsten for the group of micrococci causing inflammation, was placed with tetrad-forming micrococci in the genus

Micrococcus in 1885. Staphylococci were delineated from micrococci a year later, in 1886, giving rise to the generas *Staphylococcus, Micrococcus,* and *Planococcus* in the Micrococcaceae family. Further advances in the differentiation of staphylococci from micrococci were proposed based upon their respective dependency for oxygen, with facultatively anaerobic cocci placed in the genus *Staphylococcus*, and obligate aerobic cocci placed in the *Micrococcus* genus (Götz *et.al.*, 2006). Cell-wall composition, menaquinone pattern, antibiotic susceptibility, DNA-DNA and DNA-RNA hybridization studies, and comparative 16S rRNA sequence analysis can all be employed to differentiate and identify members of the *Staphylococcal* genus (Götz *et.al.*, 2006; Kloos, 1980). Recently, taxonomic studies analyzing the species of the genus *Staphylococcus* have indicated the existence of unique genealogical groups, as represented by the species *Staphylococcus epidermis, Staphylococcus saprophyticus, Staphylococcus simulans, Staphylococcus intermedius, Staphylococcus hyicus, Staphylococcus sciuri, Staphylococcus aureus* and *Staphylococcus caseolyticus* (Figure 1.1) (Takahashi *et.al.*, 1999).

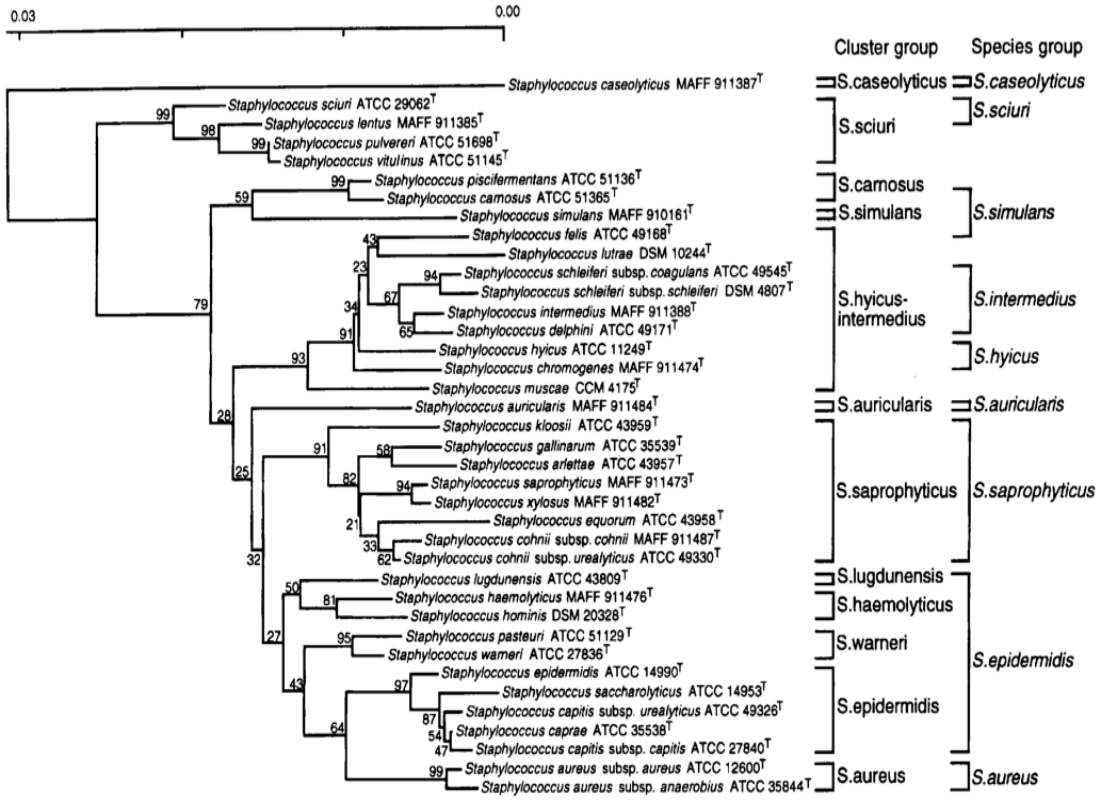

Figure 1.1 Neighbour-joining tree determined by 16S rRNA gene sequences showing phylogenetic relationships between *Staphylococcus* species (adapted from Takahashi *et.al.* 1999). The species of the *Staphylococcus* genus are divided into unique subgroups, despite close relationships between most staphylococcal species. The scale bar indicates evolutionary distance between sequences; numbers indicate confidence intervals for the position of the branches as determined by bootstrap analysis. Establishment of phylogenetic relationships between staphylococcal species may provide insight on the acquisition of virulence determinants, genetic variation, and adaptation to host environment.

1.2 ***Staphylococcus aureus***

First discovered in the 1880s by Alexander Ogston, *Staphylococcus aureus* is now one of the most prevalent nosocomial pathogens, likely mediated by adaptable, flexible, and multifaceted interactions with its surroundings (Shinefield *et.al.,* 2009; Deurenberg *et.al.*, 2008). *S. aureus* can exist in both inanimate sites as well as various niches in human and animal hosts. It is considered both a commensal bacteria, inhabiting skin and mucous membranes, and a highly pathogenic one, inducing disease states in blood and tissue sites (Harraghy *et.al.*, 2007; Novick, 2003). Adding to its infection proficiency and virulence, *S. aureus* is an adept asymptomatic colonizer, with approximately 20% of the population as chronic carriers of the bacteria and 60% infected intermittently. Moreover, *S. aureus*, is the leading cause of skin and soft tissue infections (SSTIs), lower respiratory tract infections and blood stream infections world wide (Liu, 2010; Shinefield *et.al.,* 2009). In conjunction with this niche habitat and disease state versatility, *S. aureus* is under increasing risk for the development of resistance to most currently available therapeutics, providing this organism with the genetic tools and traits to produce a highly pathogenic disease agent (Mayville *et.al.*, 1999).

Methicillin resistant *S. aureus* (MRSA) is presently the most commonly identified antibiotic resistant pathogen in many parts of the world, including the Americas, north Africa, the middle east, east Asia and parts of Europe where MRSA infection levels were previously stable (Grundmann *et.al.*, 2006). Presenting by and large as nosocomial infections and occurring in conjunction with complications in health-care procedures or underlying disorders makes defining morbidity, mortality and loss of productivity as a

direct result of MRSA hard to define. In spite of this, an obvious financial and psychological burden is evident with respect to societal costs directly incurred by extended hospital stays, additional therapeutic and diagnostic procedures and indirectly through productivity loss, increased mortality, and increases in long-term disability (Lee *et.al.*, 2013; Chambers *et.al.*, 2009). With the escalating virulence and antibiotic resistance of this organism and increased disease burden, novel non-antibiotic therapeutic options are desperately needed and will be imperative for the maintenance and control of *S. aureus* infections in clinical and community settings.

1.2.1 *Staphylococcus aureus* Pathogenesis

Mediated by a vast arsenal of virulence factors, *S. aureus* is efficient at eliciting a broad range of host infections, in both physiology and severity. Clinical infections associated with *S. aureus* range from minor SSTIs to endocarditis, sepsis, and necrotizing pneumonia, affecting both healthy and immuno-compromised hosts (Lowy, 1998). As natural reservoirs of *S. aureus* humans, particularly persistent carriers of the bacteria, are already at a heightened risk for staphylococcal disease (Wenzel *et.al.*, 1995). This can further be exacerbated in patients with diabetes, intravenous drug users, hemodialysis patients, surgical patients, and immuno-compromised individuals in close quarter facilities including the military, sports teams, and penitentiaries (Gordon *et.al.*, 2008; Benjamin *et.al.,* 2007).

Colonization by *S. aureus* begins with the adherence and invasion of host epithelial cells, predimonantly those of the anterior nares, and is mediated by a group of

staphylococcal surface proteins termed MSCRAMMs (microbial surface components recognizing adhesive matrix molecules) (Gordon *et.al.*, 2008; Liu, 2009; Otto, 2012). The logarithmic phase production of these small adhesions factors promotes bacterial binding to host tissues via interactions with collagen, fibronectin and fibrogen. Persistence of staphylococcal colonization is further aided by the formation of biofilms on host tissues and prosthetic surfaces, mediating evasion of host defenses, and through the creation of small-colony variants (SCV), auxotrophic bacterial subpopulations that are able to effectively shelter in host cells whilst providing protection from antibiotics and host defenses (Gordon *et.al.*, 2008; Melter *et.al.*, 2010).

Once established, colonization situates *S. aureus* in close proximity to key mucus membranes including the throat, ears, mouth and sinus. It isn't until host skin or mucosal barriers are breached, however, that staphylococcal infection is initiated. Once exposed to tissues beyond these external surfaces, *S. aureus* undergoes a fundamental density-dependent phenotypic switch resulting in the downregulation of tissue adherence factors and up-regulation of virulence factors (Liu, 2009; Rothfork *et.al.*, 2003). Mediated in part by the quorum sensing (QS) accessory gene regulator (*agr*), this switch is predominately responsible for the onset of virulence and staphylococcal-specific pathologies seen with *S. aureus* infections (Gordon *et.al.*, 2008). Proteases, lipases, and elastases enable the invasion and destruction of host tissues, allowing *S. aureus* to metastasize to auxiliary sites. In the process, staphylococcal superantigens, including hemolysins and toxic shock syndrome toxins, are generated and secreted resulting in the mobilization of the host immune system and coagulase pathways (Gordon *et.al.*, 2008). The hallmark

staphylococcal diseases resulting from *S. aureus* infection include toxic shock syndrome, sepsis, metastatic infections of the bones, joints, kidneys and lungs, endocarditis and bacteremia (Lowy, 1998). While the armamentarium of *S. aureus* virulence factors is extensive, the spread of staphylococcal infection is dependent on an intricate interaction between bacterial virulence factors, immune evasion and innate host defense mechanisms.

1.2.2 Antibiotic Resistance in *Staphylococcus aureus*

Antibiotics have undoubtedly exerted the most concentrated selective pressure on *S. aureus* during the organism's long co-evolution with man, and in conjunction with horizontal and vertical gene transfer, have dramatically altered the antibiotic resistance landscape of the staphylococcal genome. Infection by antibiotic resistant strains of *Staphylococcus aureus* have become globally epidemic and the burden of staphylococcal disease in both health care and community settings continues to increase (Chambers *et.al.*, 2009).

The frequency of antibiotic resistance among staphylococcal bacteria has increased rapidly since the introduction of antibiotic therapeutics for the treatment of bacterial infections in the 1940s (Duerenberg *et.al.*, 2008). The first major antibiotic resistance event in the history of *Staphylococcus* infections was acquired resistance to penicillin, a clinical occurrence that was combated by the introduction of methicillin in 1959. By 1961, there were reports from the United Kingdom of methicillin resistant *S. aureus* (MRSA) isolates, followed shortly thereafter by similar discoveries in Japan, Europe, Australia and the United States (Enright *et.al.*, 2002; Grundmann *et.al.*, 2006).

Currently there exist three major antibiotic resistance strains of *S. aureus*: MRSA, vancomycin-intermediate *S. aureus* (VISA), and vancomycin-resistant *S. aureus* (VRSA); each of which is becoming increasingly difficult to combat due to emerging resistance of *S. aureus* to all current antibiotic classes (Enright *et.al.*, 2002).

Methicillin-resistant *Staphylococcus aureus* has long been deemed a predominately hospital acquired infection (HA-MRSA), with risk factors including recent surgery or hospitalization, residence in a long-term care facility, dialysis, and indwelling percutaneous medical devices and catheters (Vandenesch *et.al.*, 2003). Recently, however, cases of MRSA in healthy community-dwelling individuals with no underlying risk factors have been identified, indicating the changing epidemiology of the MRSA infection (Moellering Jr, 2012; Hawkey *et.al.*, 2009). Community-associated MRSA (CA-MRSA), characterized by the presence of the toxin Panton-Valentine leukocidin, is one of the leading causes of skin and soft tissue infections, giving rise to a range of physiological disease states from mild cellulitis and abscesses to necrotizing fasciitis, necrotizing pneumonia, bone and joint infections, infections of the nervous system, and bacteremia and endocarditis (Chambers *et.al.*, 2009; Yao *et.al.*, 2010). These strains are genetically unrelated to previously identified hospital-associated infections. USA300, the most predominant CA-MRSA strain, has tripled in prevalence since 2004, and appears to be more biologically fit than its MRSA counterparts. Additionally, recent reports have highlighted the influx of USA300, and CA-MRSA mediated bacteremia, in nosocomial infections (Rehm, 2008; Hawkey *et.al.*, 2009).

The cause of resistance to methicillin and all other β-lactam antibiotics lies within the *S. aureus mecA* gene, situated on a mobile genetic element termed the staphylococcal cassette chromosome *mec* (SCC*mec*) (Chua *et.al.*, 2013). The methicillin-resistance determinant *mecA* encodes a 78 kDa penicillin-binding protein (PBP2A) that acts as a transpeptidase, and assisted by the transglycosylase domain of native *S. aureus* PBP2 continues synthesis of the peptidoglycan cell wall layer. In the absence of *mecA* and its gene product PBP2, β-lactam antibiotics bind to native penicillin binding proteins (PBP) in the *S. aureus* cell wall and disrupt biosynthesis of the peptidoglycan layer resulting in cell death (Deurenberg *et.al.*, 2008; Grundmann *et.al.*, 2006). Five types of SCC*mec* (SCC*mec* I to V) and several variants have been described based on the combinations of the *mec* gene complex and cassette chromosome recombinases (*ccr*) genes, which integrate and excise SCC*mec* into and out of the *S. aureus* genome at the SCC*mec* attachment site (Ito *et.al.*, 2001; Grundmann *et.al.*, 2006; Deuruenberg *et.al.*, 2009). The origins and mechanism of transfer of SCC*mec* are still unclear and at present no other bacterial isolates of other genera have been shown to carry this element (Grundmann *et.al.*, 2006). Antibiotic resistance afforded by presence of the SCC*mec* element in conjunction with inter- and intra-species communication associated with virulence, intracellular survival and biolfilm formation, exert a concerted effect on staphylococcal pathogenicity, making new infections and ever evolving strains more difficult to treat.

1.2.3 *Staphylococcus aureus* Genetics

The staphylococcal genome consists of a 2.8 Mb circular chromosome, with prophages, plasmids and transposons. A core set of 1,681 open reading frames contain genes governing virulence, antibiotic resistance, and extrachromosomal elements (Lowy, 1998; Gill *et.al.*, 2005). In 2001, the whole genome sequences of two *S. aureus* reference strains, the methicillin-resistant N315 and vancomycin-resistant Mu50, were published and since then over 28 whole genomes have been sequenced, annotated and made publicly available (Kuroda *et.al.*, 2001; Hecker *et.al.*, 2010; Chua *et.al.*, 2013).

The *S. aureus* genome is comprised of a conserved 2.3 Mb core genome, encoding fundamental housekeeping genes, conserved virulence determinants, and genes required for bacterial growth (Lindsay *et.al.*, 2004). Conversely, a variable accessory genome encompasses mobile genetic elements (MGEs) including transposons, plasmids, insertion sequences, integrated bacteriophages, and pathogenicity islands. These hypervariable regions encode genetic determinants for the phenotypic behaviour of individual bacterial subpopulations, including antimicrobial resistance genes, exotoxins, superantigens and effectors of host immune responses (Chua *et.al.*, 2013; Hecker *et.al.*, 2010). Augmenting the instability of genetic elements within the accessory genome is preliminary evidence suggesting that some of these components may readily move between isolates at high frequency, while others are stationary or shift infrequently. The transfer and carriage of these MGEs can drastically alter the pathogenic and resistance phenotypes of *S. aureus* strains, but require MGE-specific excisonases, independent replication, and integration

mechanisms during transduction to competently circumvent the restriction deficient phenotype of most strains (Lindsay, 2010; Lindsay *et.al.*, 2004).

Notorious for difficulties in laboratory-based genetic manipulation, as illustrated by the rejection of exogenous plasmids, *S. aureus* strains are by-and-large restriction deficient (Feng *et.al.*, 2008).The Sau1 type I restriction modification system, found in all strains of *S. aureus*, is composed of a single *hsdR* (restriction subunit) gene, two copies of *hsdM* (modification subunit) genes, and two variable copies of *hsdS* (sequence genes). The combination of *hsdS* genes differs between *S. aureus* lineages, allowing for the identification and immediate digestion of foreign DNA. The HsdM and HsdS subunits recognize and modify bacterial host DNA, or DNA from the same *S. aureus* lineage, protecting it form digestion (Lindsay, 2010; Waldron *et.al.*, 2006). The *S. aureus* cloning intermediate strain RN4220, is the only restriction-deficient strain known to date, and serves as a vital tool for genetic manipulation. First identified in 1983, the chemical mutagen of 8325-4, RN4220 can readily accept *Escherichia coli*-propagated plasmids by electroporation due to a *hsdR* mutation (Kreiswirth *et.al.*, 1983).

Multi-locus sequence typing has revealed the highly clonal population structure of *S. aureus*, where drastic recombination events are notably rare occurrences. Of the numerous clonal complexes possible, 87% of *S. aureus* found in hospital and community settings belong to a subset of 11 clonal complex groups, suggesting preferential carriage of accessory genes with benefit to survival or virulence by several clonal complexes (Chua *et.al,* 2013; Feil *et.al.*, 2003). These findings highlight the importance of continued genomic research in the discovery of the evolution and adaptation of *S. aureus* species to

acquire antibiotic resistance and alter virulence phenotypes, ultimately revolutionizing the understanding, maintenance and treatment of staphylococcal related infection.

1.3 Bacterial Quorum Sensing

Over the last two decades, the convention that prokaryotic existence is defined by unicellular organisms in a bacterial population operating as autonomous units has been dismissed, superseded with understanding that social interactions are common throughout both the eukaryotic and prokaryotic world (Reading *et.al.*, 2006; Atkinson *et.al.*, 2009). It is now realized that, while once considered primarily selfish, numerous bacteria utilize a sophisticated communication network to coordinate collective behaviours in response to environmental challenges (Atkinson *et.al.*, 2009; Miller *et.al.*, 2001). The first discovery of bacterial cell-to-cell communication occurred in 1970 in the luminous marine bacterium *Vibrio fishceri*. Kenneth H. Nealson and John W. Hastings of Harvard University observed that bacterial fluorescence only occurred at high population densities and postulated that bioluminescence was regulated by diffusible molecular messengers, termed "autoinducers", that entered target cells and activated genes involved in bioluminescence (González *et.al.*, 2006; Raina *et.al.*, 2009; Turovskiy *et.al.*, 2007). Over twenty years later, in 1994, this process of bacterial cell-to-cell communication was termed "quorum sensing" (QS) and has since been shown to be a widespread mechanism of gene regulation in both Gram positive and Gram negative bacteria (Reading *et.al.*, 2006; Turovskiy *et.al.*, 2007).

Quorum sensing permits population-dependent adaptive behaviours through monitoring the presence of other bacterial cells and regulating gene expression in response to changes in population density and environmental cues (Rutherford *et.al.,* 2012). In the most basic scenario, bacteria produce autoinducers, the diffusible QS signal molecule, which accumulate to a threshold autoinducer concentration, correlated with an increasing population density. Once this threshold has been reached, activation of a signal transduction cascade is initiated culminating in a population-wide expression or repression of target genes and resulting in a synchronized behavioural adaptation (Taga *et.al.*, 2003; Waters *et.al.*, 2005; Camilli *et.al.*, 2006). Most QS regulated behaviours are productive only in response to the concerted action of numerous cells, with such QS-controlled processes including bioluminescence, biofilm formation, virulence factor expression and secretion, sporulation, conjugation, antibiotic production and pigment production (Taga *et.al.*, 2003; Camilli *et.al.*, 2006). As a result of the synchronized responses that are mediated through quorum sensing, bacteria are able to take on some of the characteristics of multicellular organisms (Bassler, 2002).

There are two archetypal quorum sensing circuits characterized to date (Figure 1.2), with differences in the systems likely present as a result of optimization to promote survival and pathogenesis of different bacterial species within their specialized niches (Reading *et.al.*, 2006; Bassler, 2002) .

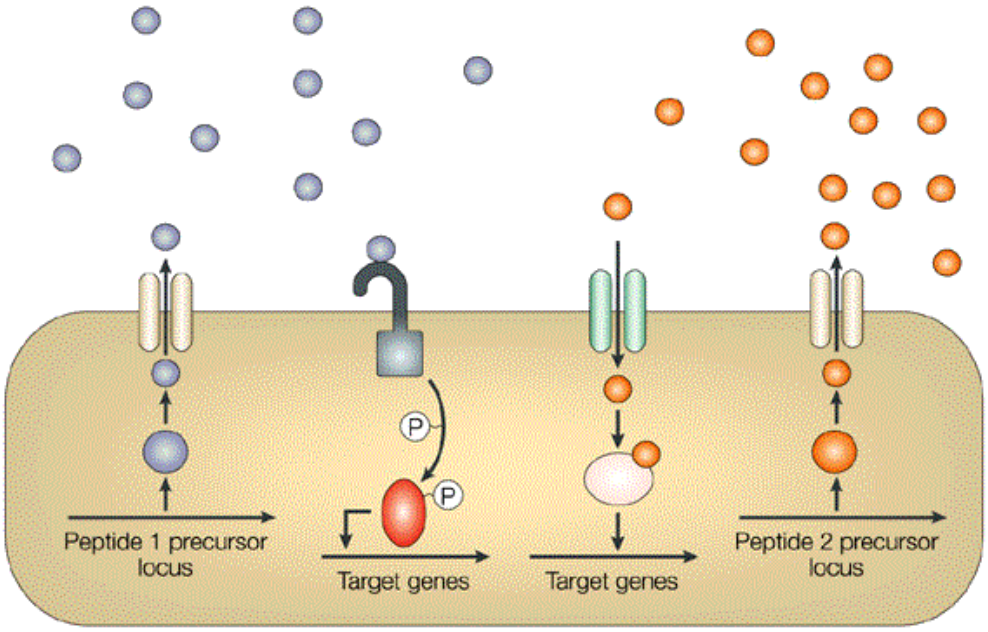

Figure 1.2: The quorum-sensing pathways in Gram-positive and Gram-negative bacteria (adapted from Lazdunski *et.al.*, 2004). Gram-positive bacteria (pictured left) employ small oligopeptide signaling molecules, termed AIPs (light grey), to activate the quorum sensing circuit. AIPs are synthesized as precursor peptides, which are processed, modified and exported via an adenosine triphosphate (ATP)-binding cassette transporter (yellow). As the bacterial cell population density increases, so too does the concentration of the secreted autoinducer. Peptide binding to a membrane-bound TCSK (dark grey) stimulates intrinsic autophosphorylation and downstream phosphor-transfer, resulting in the activation of the cognate response regulator (red), which in turn regulates the transcription of target genes. In Gram-negative quorum sensing (pictured left), following production AHL autoinducer molecules (orange) diffuse out of and into bacterial cells, or may be assisted by membrane-bound permeases (green). At critical threshold concentrations, the AHL is bound by the response regulator (pink), which triggers transcription of downstream quorum-sensing regulated genes.

1.3.1 Quorum Sensing in Gram-Negative Bacteria

The simple signal-response mechanism first recognized by Nealson and Hastings in *V. fischeri*, and later described by Joanne Engebrecht and Michael Silverman (1984) has now been identified in over 25 species of Gram-negative bacteria for the control of cell-density dependent functions (Bassler, 1999; Miller *et.al.*, 2001). These systems specifically, contain at minimum homologs of two *V. fischeri* regulatory proteins termed LuxI and LuxR. (Miller *et.al.*, 2001; Taga *et.al.*, 2003). LuxI is the autoinducer synthase that catalyzes the synthesis of a specific acyl-homoserine lactone (AHL) autoinducer. LuxI produces AHLs by linking acyl chains from lipid metabolism, carried by acyl-acyl carrier proteins, to the homocysteine moiety of *S*-adenosylmethionine. AHLs contain a conserved homoserine lactone ring with variable acyl-side chain moieties (Taga *et.al.*, 2003; González *et.al.*, 2006). Acyl side chains vary in the number of carbons from 4 to 18 with the potential for modification (hydroxylation, carbonyl group addition, or full reduction) at the C-3 position, allowing for variation and ensuring specificity of interaction with LuxR-type proteins (Reading *et.al.*, 2005; González *et.al.*, 2006). LuxR and like proteins are transcription factors, which upon recognition and binding of the cognate AHL autoinducer, associate with the *luxICDABE* promoter and activate transcription of luciferase enzymes encoded by the operon (Miller *et.al.*, 2001; Taga *et.al.*, 2003). AHL binding to LuxR stabilizes these proteins and unmasks the LuxR DNA binding domain; in the absence of a signal LuxR and like proteins are targeted for degradation (Reading *et.al.*, 2006; Zhang, 2002; Miller *et.al.*, 2001). The carboxy-terminal domain of each LuxR homolog contains a highly conserved helix-turn-helix

motif that mediates binding to a 20-base pair palindromic DNA sequence termed the "lux box". Because of the conserved nature of DNA-recognition elements in LuxR proteins it has been suggested that inherent target specificity in these systems is derived from the selectivity of LuxR proteins for their corresponding autoinducer (Miller *et.al.*, 2001). Specificity in the LuxR-AHL interaction is critical to the organism's ability to distinguish AHLs produced by their own species from those produced by other bacterial species (Taga *et.al.*, 2003). Among the 25 bacterial species that utilize the LuxI/LuxR-type circuit for quorum sensing, *V. fischeri, Pseudomonas aeruginosa, Agrobacterium tumefaciens* and *Erwinia carotovora* are the best understood (Miller *et.al.*, 2001).

1.3.2 Quorum Sensing in Gram-Positive Bacteria

Quorum sensing in Gram-positive bacteria relies on signaling by small oligopeptide autoinducers, which interact with two component sensor kinase (TCSK) systems to regulate gene transcription in response to cell population density. The small peptide autoinducers are produced from propeptide precursors that are cleaved or further modified prior to bacterial export (Reading *et.al.*, 2006; Bassler, 1999). These autoinducing peptides (AIPs) range from 5 to 17 amino acids in length and are often post-translationally modified by the addition of thiolactone and lactone rings, lathionines and isoprenyl groups (Camilli *et.al.*, 2006). Synthesis of AIPs is inherently accurate as signal generation is directly dependent upon the specific DNA sequence encoding the precursor peptide (Taga *et.al.*, 2003). Similar to other QS subtypes, peptide QS signaling molecules exhibit high specificity for their cognate receptors. Unlike AHL autoinducing molecules

however, AIPs are not diffusible, and thus rely on secretion by a dedicated ATP-binding cassette transporter (Miller *et.al.*, 2001; Reading *et.al.*, 2006; Waters *et.al.*, 2005). Increases in cell density occurs concomitantly with an increase of secreted AIPs until a threshold AIP concentration is reached in the extracellular environment. At threshold concentrations the AIP binds to a cognate TCSK in the bacterial membrane. Interaction with the peptide ligand instigates a series of phosphorylation events by the membrane-bound sensor kinase including the initiation of a phospho-transfer to the cytoplasmic response regulator (Ng *et.al.*, 2009). The phosphorylated, and thus activated, response regulator binds DNA and alters transcription of the targeted genes (Bassler, 1999; Miller *et.al.*, 2001).

Bacterial processes among Gram-positive organisms that are controlled by cell population density include competence for DNA uptake, virulence, conjugation and microcin production. The signaling substructure that mediates each of these processes is the same; however variations do occur with respect to the addition of alternative regulatory factors. *Bacillus subtilis* for example, utilizes two processed peptide signals that allow the bacteria to select between competence for DNA uptake or sporulation (Bassler, 1999). At threshold concentrations, ComX, the characteristic Gram-positive QS molecule, is detected by the ComP/ComA TCSK system. Phosphorylated ComA induces the expression of *comS*, and functional ComS protein inhibits the proteolytic degradation of ComK. ComK is a transcriptional regulator that controls the expression of competence related genes and thus this regulatory pathway commits cells to a competence pathway. The second peptide, the pentapeptide CSF, inhibits compentence at high concentrations

while simultaneously promoting the bacterial sporulation pathway through an indirect increase in the sporulation-stimulating response regulator Spo0A (Ng *et.al.*, 2009; Magnuson *et.al.*, 1994).

1.4 Quorum Sensing in *Staphylococcus aureus*

The versatility of *S. aureus* antibiotic resistance, colonization and pathogenesis is dependent upon an intricate network of adaptive and accessory gene systems. Of the approximately 50 accessory genes that encode for pathogenesis related proteins, most correspond to proteins that are displayed on the bacterial surface or released into the surroundings enabling the organism to evade host defenses, adhere to cells, to spread within the host, and to degrade cells and tissues. The vast majority of these critical exoproteins are controlled by a global accessory gene regulator termed *agr* (Novick, 2003). Like most other bacterial species, the genes comprising the virulon are regulated in a highly synchronized manner depending upon the biological needs of the organism, tying *agr* regulation of gene transcription directly to quorum sensing (Novick *et.al.*, 2008; Harraghy *et.al.*, 2007).

The *agr* locus encodes a two-component signal-transduction system and characteristic autoactivation circuit (Novick *et.al.*, 2003; Chen *et.al.*, 2009). The ≈3 Kb locus is expressed from two divergent promoters, P2 and P3, with P2 encoding 4 genes for *agrB, D, C* and *A*. The two component-sensor histidine kinase (HK) is composed of ArgA, a response regulator, and ArgC, the polytopic transmembrane receptor and sensor histidine kinase. AgrB and D function synergistically to form the processed autoinducing

peptide. Once released, and at threshold concentrations, the AIP binds to and activates AgrC, mediating the phosphorylation and activation of AgrA. Activated AgrA promotes expression of the P2 promoter thereby upregulating expression of the *agr* locus for the amplification of AIP production. AgrA also simultaneously promotes expression of the divergent P3 promoter and its RNAIII transcript. RNAIII is the regulatory effector of the circuit and modulates expression of *S. aureus* toxin genes and secreted surface proteins in relation to cell density defining the *agr* phenotypic switch (Novick *et.al.*, 2003; Geisinger *et.al.*, 2009; Chen *et.al.*, 2009) (Figure 1.3). Phenotypic switching occurs as a direct result of the *agr* system, during which alterations in expression patterns shift the bacteria from an early establishment phase to a late virulence phase. Early in bacterial growth genes encoding surface proteins are downregulated, whereas those encoding secreted proteins, including bacterial toxins, are upregulated post-exponentially (Dunman *et.al.*, 2001).

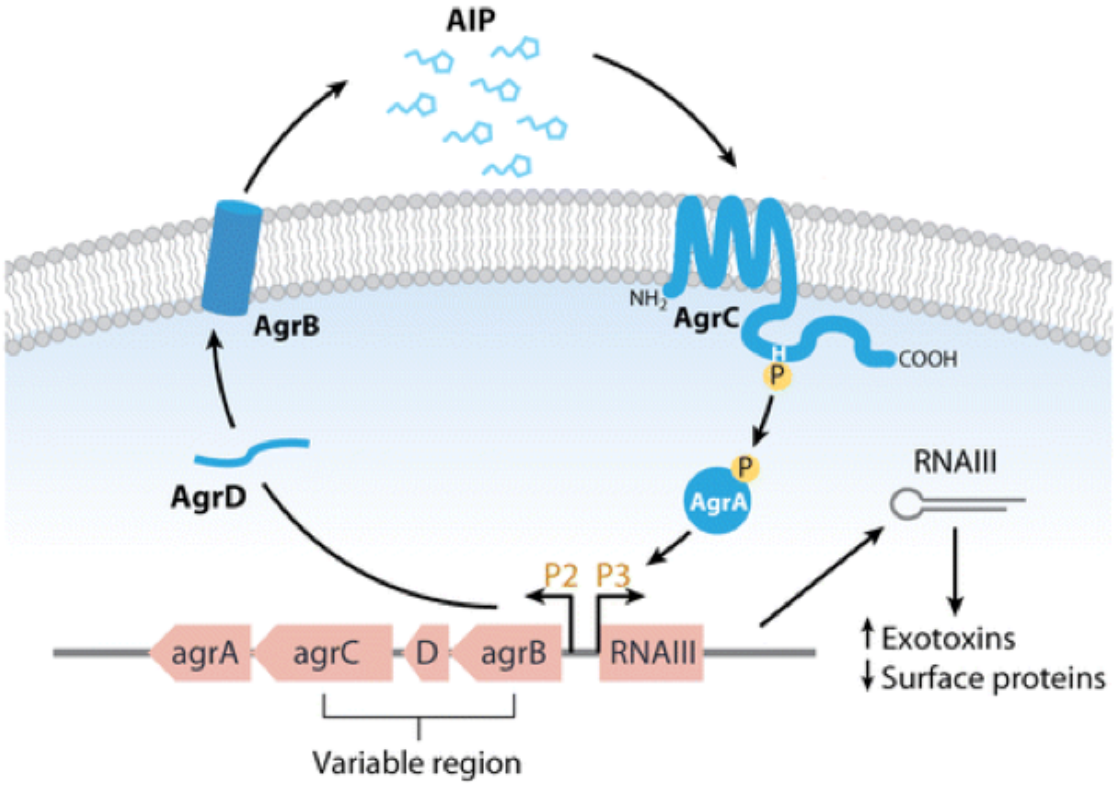

Figure 1.3: The *agr* autoactivation circuit (adapted from Novick *et.al.*, 2008). The AgrD peptide precursor is processed at N-terminal and C-terminal cleavage sites by the transmembrane endopeptidase AgrB. Mature AIPs are secreted in the form of a thiolactone ring with a 2-5 amino acid tail, which binds to and activates the transmembrane receptor domain of the sensor kinase AgrC. Ligand binding induces phosphorylation of the cytoplasmic HK domain and a subsequent phosphorelay of the phosphate to AgrA. Activated, phosphorylated AgrA activates transcription from the two divergent *agr* promoters, P2 and P3. The P2 promoter drives autoactivation circuit expression, while the P3 promoter drives transcription of RNAIII, the regulator effector and induces *agr* phenotypic switching.

1.4.1 *Agr* Specificity Groups

Allelic variations in the *S. aureus agr B-D-C* region have resulted in the emergence of four *agr* specificity groups (groups I through IV). The basis for these variations is unknown but is hypothesized to mediate quorum-sensing interference between different *agr* group strains, prompting *S. aureus* strain segregation and divergence (Novick *et.al.*, 2008; Geinsinger *et.al.,* 2012). The groups are defined by heterologous mutual inhibition, during which peptides of each group will cross-inhibit the *agr* response in strains of heterologous groups. This bacterial interference is novel in that the *agr* regulon and not bacterial growth is inhibited (Ji *et.al.*, 1997; Novick *et.al.*, 2008). The ability of an AIP to activate its cognate receptor is highly sequence specific, thus a change in a single amino acid can alter group specificity. As a result, the propeptide *agrD* sequence variants directly correlate to *agrC* sequence variants, a concerted evolution ensuring AIP-AgrC sequence specificity and finite *agr* activation (Novick, 2003). The N-terminal one-third of *agrB* and C-terminal histidine protein kinase domain (HPK) of *agrC* are highly conserved, with a hypervariable region occurring in the intervening sequences as indicated in Figure 1.3. These highly divergent regions are the primary determinants of group specificity.

Interestingly, allelic variation within the *agr* operon is not mutually exclusive to *S. aureus*, and at least 15 other staphylococcal species examined thus far display unique *agr* locus variants, several of which have exhibited heterologous inhibition on the *S. aureus agr* (Dufour *et.al.,* 2002; Novick, 2003; Geisinger *et.al.*, 2009). Moreover, *S. aureus* specificity groups exhibit prominent differences in infection type, suggesting that *agr*

specificity groups may also modulate strain virulence and pathogenicity. *S. aureus agr* group III strains, for example, are predominantly associated with menstrual toxic shock syndrome and are the most frequent underlying cause of Panton-Valentine leukocidin-associated necrotizing pneumonia (Geisinger *et.al.*, 2012; Tristan *et.al.*, 2007). Most exfoliatin-producing strains, responsible for staphylococcal scalded skin syndrome, are of the *agr* group IV classification, while VISA strains belong to *agr* group II (Jarraud *et.al.*, 2002; Novick, 2003). While MGEs undoubtedly play a significant role in the acquisition of staphylococcal virulence determinants, the underlying molecular basis for these patterns in biotype specficity are currently unknown. It can be hypothesized however, that linkage disequilibrium between MGEs carrying these virulence determinants, or *agr* group-specific selective factors regulating their transmission may be governing factors (Novick *et.al.,* 2008).

1.4.2 AIP Synthesis, Processing and Structure

AgrD encodes the peptide precursor sequence that must undergo both N- and C-terminal processing to produce the mature 7-9 amino acid AIP. It is a membrane protein, anchored in the inner leaflet of the cytoplasmic membrane by an N-terminal amphipathic α-helix, promoting specific interaction of the C-terminal region with the AgrB endopeptidase (Qiu *et.al.*, 2005; Novick *et.al.*, 2008). The mature peptide consists of a cyclic thiolactone, hallmark of these peptides and essential for AIP activity, that is formed between the sulfhydryl group of a conserved central cysteine 5 amino acids from the C-terminus and the peptide's C-terminal carboxyl group (Mayville *et.al.*, 1999; Qiu *et.al.*,

2005; Novick *et.al.*, 2008). Structure-function analysis of AIPs I and II demonstrate that replacement of the thiolactone ring by a lactone or lactam bond eliminates activation but not heterologous inhibition of the peptide, while removal of the tail region converts the oligopeptide into a universal inhibitor of *agr* function (Novick, 2003). The AIP inhibition of AgrC function is strictly competitive suggesting that inhibitory peptides reversibly block access to the AgrC receptor activation site (Lyons *et.al.,* 2002).

Unlike the AIP-AgrC interaction, the group specificity of AgrD processing by AgrB is less stringent and AgrB-I and AgrB-III will each process AgrD-I and AgrD-III with equal proficiency, but neither will process AgrD-II or AgrD from other staphylococcal species (Novick, 2003; Novick *et.al.*, 2008). The AIP sequence in the AgrD propeptide is centered between the N-terminal α-helix and a highly hydrophilic C-terminal region. The processing of the propeptide to mature AIP requires two processing steps, formation of the thioester bond and secretion, and the activity of the transmembrane endopeptidase, AgrB (Qiu *et.al.*, 2005; Novick *et.al.*, 2008). AgrB cleaves the AgrD propetide at its C-terminal processing site in a reaction involving the conserved residues histidine 77 and cysteine 84, the latter of which likely catalyzes the formation of the thiolactone ring and displacement of the peptide from AgrB (Qiu *et.al.*, 2005). Once processed, the AIP-precursor (N-terminal leader fused to AIP) is transported to the outer leaflet of the cell membrane via an unknown mechanism, where type I signal peptidase SpsB removes the N-terminal amphipathic helix completing the AIP processing pathway (Thoendel *et.al.*, 2009; Kavanaugh *et.al.*, 2007). AIPs-I and IV are octapeptides, AIP-II is a nonapeptide and AIP-III is a heptapeptide (Figure 1.4) (Novick, 2003).

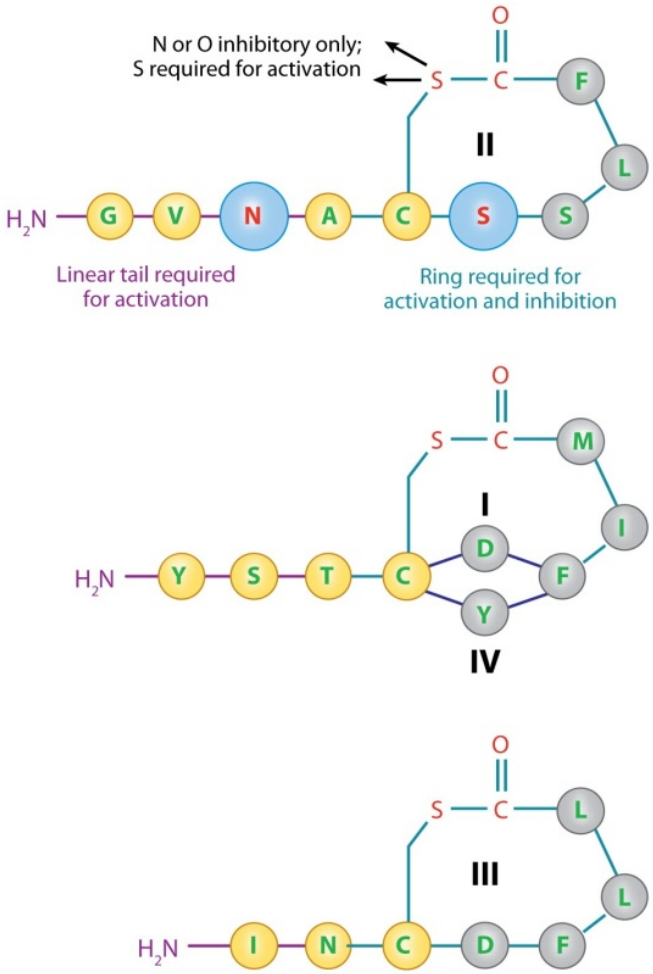

Figure 1.4: *S. aureus* AIP Structure (adapted from Novick *et.al.*, 2008). Diagram of the four *S. aureus* AIP specificity groups. Two key residues of the nonapeptide AIP-II are shown in blue. AIP-I and AIP-IV differ only at a single site. Replacement of the conserved cysteine generates cross-inhibitory peptides that are inactive with their cognate receptor.

1.4.3 AgrC: the Sensor Kinase and Signal Receptor

Quorum sensing signaling with respect to the *agr* locus depends upon signal transduction by the polytopic transmembrane receptor and sensor kinase AgrC. The N-terminal transmembrane sensor domain is required for AIP recognition and signal transduction as is demonstrated by the construction of chimeric AgrC proteins with altered sensor domains (Geisinger *et.al.*, 2008; Novick *et.al.*, 2008). Switching the proximal and distal portions of the N-terminal receptor domain of AgrC proteins localizes the specific recognition of AIPs to the distal subdomain. The response of the functional chimeras to different AIPs suggests that AgrC loop 2 is critical for AIP discrimination and activation of signal transduction (Wright *et.al.,* 2004; Novick *et.al.*, 2008). While the C-terminal sub domain contains highly conserved transmembrane helices 3, 5 and 6 and extracellular loop 3, it is unlikely that this domain is involved in AIP discrimination due to the high sequence similarity present between *agr* subgroups, and is likely involved in transmission of the ligand-induced signal to the histidine-protein-kinase domain (HPK) (Novick *et.al.*, 2008).

Upon external environmental signals, the preformed homodimeric AgrC binds cognate thiolactone AIPs via its N-terminal transmembrane sensor domain (Geisinger *et.al.*, 2008; Novick *et.al.*, 2008). The general model of AIP receptor interaction suggests that two key distinct events occur. Firstly, the peptide enters a hydrophobic pocket of the receptor in a non-sequence specific manner, necessitating the two bulky C-terminal residues of the AIP. Subsequently, the AIP makes several specific hydrophilic contacts with unique sites in the receptor, likely within the AgrC transmembrane helix 2, which

has been shown to be critical for AIP discrimination and activation of signal transduction (Novick, 2003). Cognate ligand binding, as described above, to one or both transmembrane sensor domains of the AgrC homodimer stabilizes an active conformation in the corresponding cytoplasmic catalytic core (George Cisar *et.al.*, 2009).

In prototypical histidine kinases the cytoplasmic kinase core consists of two unique subdomains: a highly conserved C-terminal catalytic and ATP-binding (CA) domain, and the more variable dimerization and histidine phosphotransfer (DHp) domain (Casino *et.al.*, 2010; Perry *et.al.*, 2011; Gao *et.al.*, 2009). The DHp domain, specifically, provides an α-helical binding interface that mediates dimerization of the kinase core and contains the H-box, which houses the phosphorylation site (His239). These intermolecular interactions across the coiled-coil dimer interface induce functionally parallel conformations. This concerted establishment of activated conformational states in both protomers promotes a transautophosphorylation event mediated by the CA domains (George Cisar *et.al.,* 2009; Gao *et.al.*, 2009). As expected, a substantial interface exists between the CA and DHp domains allowing efficient and precise activation or inhibition of down stream signaling cascades based on the activation state of the sensor kinase (Gao *et.al.*, 2009). Each CA domain hosts one ATP molecule between a characteristic ATP-lid and central helix. The ATP-lid is suggested to undergo structural shifts based on the step of the phosphorelay process with respect to the phosphoacceptor His residue. (Perry *et.al.*, 2011, Gao *et.al.*, 2009).

Upon ligand binding the cognate signal is transduced via conformational changes. These conformational changes are conferred by tilting and rotational movements in

helical domains directly adjacent to the kinase core, resulting in the subsequent rotation and bending of the DHp domain. Such movements allow the CA domain to move nearer or further away, permitting either the alignment of the ATP molecule with histidine for kinase reaction or presenting a docking site for the response regulator in phosphotransfer reactions. Once phosphorylated, the H-box histidine is poised to participate in phosphotransfer reactions necessary for the activation of the response regulator (Casino *et.al.*, 2010; Gao *et.al.*, 2009).

1.4.4 AgrA and RNAIII: the Response Regulator and System Effector

AgrA is the response regulator of the *S. aureus* quorum sensing system and is required for the activation of the two divergent *agr* promoters, P2 and P3 (Koenig *et.al.*, 2004). At a molecular level, AgrA contains a conserved regulatory receiver (REC) domain that participates in catalysis of phosphotransfer from the HK to itself and subsequent regulation of effector domain activity based on phosphorylation state. The AgrA REC domain binds to its partner protein, AgrC, by association with helix 1 of the DHp domain posterior to the H-box histidine. The resulting conformation places the ArgA phosphoaccepting aspartate residue in close proximity to the His-phosphodonor (Casino *et.al.*, 2010; Gao *et.al.,* 2009; Stock *et.al.,* 2000). The activated phosphoryl group from the HK histidine is then transferred to the cognate response regulator on a conserved Asp residue, generating a high-energy acyl phosphate. It is thought that the energy within the acyl-phosphate bond drives a conformational change in the AgrA REC domain leading to effector activation (Perry *et.al.*, 2011; Gao *et.al.*, 2009). Effectively, a

conformational change occurs within the C-terminal LytTR DNA binding domain, in conjunction with the formation of an AgrA dimer. This novel structure, consisting of a 10-strand β-fold, intercalates into successive major and minor grooves of the DNA binding site (Sidote *et.al.,* 2008). These DNA-AgrA interactions occur at a unique genetic element consisting of a pair of direct repeats with the consensus sequence [TA][AC][CA]GTTN[AG][TG], separated by a 12-13 base pair spacer region (Koenig *et.al.*, 2004). Two of these elements are found in the intergenic region between the *agr*P2 and RNAIII P3 promoter (Novick *et.al.*, 2008). This preference for P2 autoactivation increases the production of AIP signaling molecules, thus acting to propagate bacterial quorum sensing in a more fastidious manner.

The immediate consequence of *agr* activation is the production of the 514-nt RNAIII intracellular effector. RNAIII is stable, with a half-life of greater than 45 minutes, highly abundant, and has a complex secondary structure that is conserved among several staphylococcal species. RNAIII directly encodes an amphipathic 26-amino acid peptide, δ-hemolysin, and acts to reciprocally regulate gene expression giving rise to the previously mentioned *agr* phenotypic switch (Novick, 2003; Novick *et.al.*, 2008; Benito *et.al,* 2000). As the master regulator of *agr* quorum sensing, the sole function of RNAIII is that of an antisense translational regulator of individual exoproteins and pleiotropic regulators. It directly upregulates translation of most virulence related extra cellular proteins, such as α-hemolysin, by countering a translation-blocking secondary structure within the *hla* mRNA, and downregulates surface proteins such as protein A by pairing with translation-initiation regions (Novick *et.al.*, 2008). It is thought that translation

inhibition by RNAIII involves transcript cleavage, rendering repression irreversible (Geinsinger *et.al.*, 2006).

RNAIII-dependent gene regulation and stimulation of *agr* autoinduction by AgrA are the fundamental consequences of AIP-initiated *agr* signaling in response to cell population density. These proteins work to regulate the expression of genes involved in virulence and tissue degradation at late stages of infection where *S. aureus* populations are high enough to elicit an impactful physiological attack through the release of hemolysins and other pathogenic proteins. At low bacterial concentrations, the organism has no biological need for synthesis of these proteins, instead favouring production of cell adhesion and surface proteins to aid colonization (Novick *et.al.*, 2008; Lowy, 1998). Quorum sensing is integral to ensure that protein production is appropriate with respect to the biological needs of the organism and valuable nutrients and energy are not being wasted in the synthesis of unnecessary proteins.

1.4.5 Temporal Program of *agr* Quorum Sensing

Increasing cell population density, and the concomitant physiological transformations, is largely mediated through the temporal organization of the facultative gene expression system. In this manner, component genes must contain regulatory sequences that are activated or repressed combinatorially in a time-dependent manner by incoming signals to ensure the maintenance of energy resources and proper alterations in cellular biotype (Novick, 2003; Queck *et.al.*, 2008). In *S. aureus*, these changes are facilitated by the *agr* quorum sensing system, which together regulates virulence and

responses to environmental changes via metabolic adaptations (Dunman *et.al.*, 2001; Queck *et.al.*, 2008; Oun *et.al.*, 2013). The temporal program and regulatory organization of *S. aureus* can be divided into three fundamental transition points, likely arising in response to intracellular signaling. The first, the transition from stationary to exponential phase, requires the activation of previously dormant metabolic and biosynthetic pathways in addition to the production of key surface and accessory proteins, likely controlled by the bacteria's innate metabolic circuitry (Novick, 2003). As the *agr* AIP reaches threshold concentrations during mid-exponential phase, the *agr* autoactivation circuit is induced promoting transcription of RNAIII. The second transition occurs between exponential and post-exponential phases, a potential consequence of reduced oxygen as a result of increase population density, and is marked by the upregulation of genes encoding secreted proteins including hemolysins, the immune evasion-assisting phenol soluble modulins, and antibiotic resistance associated genes. This drastic alteration in cell phenotype from adhesion and colonization to infection and virulence is predominantly controlled by the activities of the *agr* circuit, and thus *S. aureus* quorum sensing (Figure 1.5) (Benito *et.al*, 2001; Queck *et.al.*, 2008). The third and final transition, between post-exponential and stationary phase, is accompanied by metabolic alterations that prepare the cell for long-term survival. These changes include the downregulation of most housekeeping genes and facultative genes by mechanisms that are not well understood in *S. aureus* (Novick, 2003).

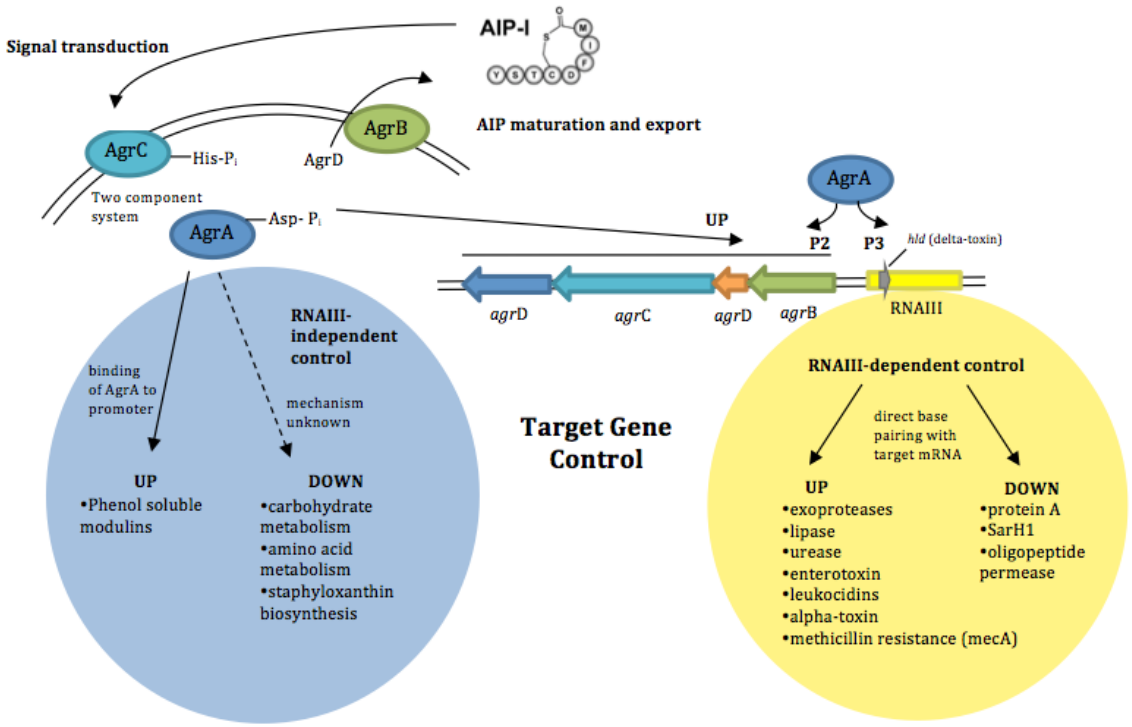

Figure 1.5: Model of target gene control by the *agr* quorum sensing circuit (adapted from Queck *et.al.*, 2008). The *S. aureus agr* quorum sensing circuit is show at the top of the image. The AIP oligopeptide is produced from the AgrD propeptide precursor protein, and processed into a 7-9 amino acid thiloactone by the endopeptidase AgrB. At threshold concentrations, the AIP binds to its cognate AgrC receptor, activating the AgrC/AgrA two component signaling system. Target gene regulation is shown in blue, for targets regulated by AgrA directly, or yellow, for targets dependent on RNAIII control.

1.5 Current Therapeutic Strategies

1.5.1 Antibiotic Therapy

The discovery of new therapeutic approaches to circumvent bacterial virulence is vital in an era when antibiotic resistance is commonplace among nosocomial and community bacterial strains. Current treatments for staphylococcal infections are limited to surgical procedures for the treatment of skin and soft tissue infections, and antibiotic therapy including the use of doxycycline, vancomycin, clindamycin and fluoroquinolones (Moellering, 2008). That being said, the use of antibiotics in the treatment of staphylococcal infections is riddled with complications and should be employed with caution. In an age where vancomycin-resistant and vancomycin-intermediate strains of *S. aureus* are emerging, vancomycin is largely still the first-line agent for antibiotic treatment of MRSA and other *S. aureus* infections (Segarra-Newnham, 2012).

Vancomycin is a bactericidal glycopeptide that displays time-dependent inhibition of cell wall synthesis in rapidly dividing cells (DiMondi, 2013; Segarra-Newnham, 2012). The Clinical and Laboratory Standards Institute have cited a minimum inhibitory concentration (MIC) breakpoint for vancomycin susceptibility at 2 µg/mL or less, however prolonged low serum concentrations of vancomycin has been associated with the onset of inducible VISA strains in patients where standard doses of vancomycin had failed. Moreover, treatment with subtherapeutic concentrations of vancomycin has been associated with the development of heterologous VISA isolate in clinical samples, highlighting the caution necessary for the employment of vancomycin as one-shot

empirical therapy for staphylococcal infections (Segarra-Newnham, 2012; Sakoulas *et.al.*, 2006).

Linezolid is the second major antibiotic to be considered, and approved by the Food and Drug Administration, for the treatment of *S. aureus* infections, particularly in cases of MRSA. It is an oxazolidinone that acts through inhibition of the 70S initiation complex assembly, and does so by binding to the 23S ribosomal RNA of the 50S subunit thereby preventing translation (Segarra-Newnham, 2012; Brink *et.al.*, 2012).. The main asset to linezolid antibiotic therapy is an astounding oral bioavailabity close to 100%, in conjunction with the absence of dose adjustment requirements in patients with renal impairment, and therapeutic drug monitoring (Segarra-Newnham, 2012; Thompson *et.al.*, 2011). As a newer therapeutic, resistance to linezolid is rare, but can occur due to mutations in the 23S rRNA peptidyl transfer domain (Brink *et.al.*, 2012). While promising, extended linezolid therapy has been associated with myelosuppression, lactic acidosis, and peripheral and optic neuropathies. The combination of high therapeutic expense, drug interaction concerns, and the aforementioned complications makes linezolid inferior in clinical efficacy as compared to vancomycin (Segarra-Newnham, 2012).

The antibiotic armamentarium to treat *S. aureus* infections, specifically those with resistance phenotypes, is limited (Table 1.1). As such, novel alternatives to antimicrobial therapy have been the focus of major research by independent laboratories and pharmacological corporations and discoveries will likely represent the new forefront of post-antimicrobial era treatment options for staphylococcal infections.

Table 1.1 Current Antibiotic Therapy for the Treatment of *S. aureus* Infection

Antibiotic	Route of administration	Main benefits	Main problems
Erythromycin	PO (main) & IV	Widespread experience of use	Comparatively poor oral absorption, GI side effects
Clindamycin	PO (main) & IV	Excellent bone penetration No monitoring required	Risk of *Clostridium difficile* diarrhoea
Linezolid	PO (main) & IV	Excellent bioavailability & tissue penetration Resistance rare	Haematological side effects limit use for long courses
Daptomycin	IV	Once daily administration Resistance rare	Necessitates IV dosing
Vancomycin	IV	Widespread experience of use	Nephrotoxicity – monitoring required Increasing resistance concerns
Teicoplanin	IV	Less nephrotoxic than vancomycin Once daily administration	Monitoring required
Doxycycline	PO	Once daily administration	GI side effects
Tigecycline	IV	Use in polymicrobial infection	
Rifampicin	PO (main) & IV	Excellent tissue penetration	Must be used in combination Extensive interations
Fusidic acid	PO (main) & IV	Excellent tissue penetration	Must be used in combination

PO, by mouth; IV, intravenous, GI, gastrointestinal.

Adapted from Thompson *et.al.*, 2011

1.5.2 Staphylococcal Vaccine Development

As an alternative to antibiotic therapy for certain patient populations displaying elevated risks for infection, disease complications and mortality, a *S. aureus* vaccine has been developed and completed both Phase II and Phase III clinical trials (Song *et.al.,* 2012). StaphVAX^{R}, a bivalent vaccine composed of *S. aureus* capsular polysaccharide types 5 and 8 conjugated to a non-toxic *Pseudomonas aeruginosa* exotoxin, displayed only partial protection for bacteremia with effects lasting no more than a few weeks in 60% of the immunized patient population (Kurlenda *et.al.*, 2012; Shinefield, 2006). While research was ultimately suspended on the StaphVAX^{R} vaccine and its derivatives, Merck is currently completing phase II clinical trials on V710, a vaccine composed of the cell-well anchored IsdB protein as the antigen. Unlike the capsular polysaccharides, IsdB is present in all clinical *S. aureus* strains and thus may present a greater trigger of immunological response and antimicrobial effectiveness (Kurlenda *et.al.*, 2012; Schaffer *et.al.*, 2008).

While these vaccines sound promising with regards to cost-effectiveness, efficacies and duration of vaccine protection, in many cases vaccine developers have in fact blatantly over stated the pharmacological activities associated with their product. To date, more often than not, clinical trials completed for *S. aureus* vaccines have done so with a failing grade despite being protective against staphylococcal infections in animal models (Bagnoli *et.al.*, 2012). Moreover, there is little evidence supporting the existence of acquired immunity to *S. aureus* infections, where recovery from infection offers no protection from subsequent infections (Schaffer *et.al.*, 2008). In some cases the

immunogen used was not appropriate with respect to its expression within major clinical isolates, or merely not well enough understood (Bagnoli *et.al.*, 2012). As an organism expressing a host of toxins and immune invasion factors, capable biofilm production, and adept immune evasion tactics, in addition to a large array of proteins and complexes with redundant functions, *S. aureus* is poised to compensate for any functions lost by a vaccine target and effectively avoid host immune responses (Goldstein, 2012; Schaffer *et.al.*, 2008). As such further *S. aureus* vaccine attempts may benefit from the production of a multivalent approach (Bagnoli *et.al.*, 2012).

1.5.3 Novel Small-Molecule and Peptide Inhibitors

As quorum sensing is employed as a virulence determinant in many bacterial strains, novel antimicrobial strategies have largely focused on the production of synthetic antagonists to the quorum sensing molecules. Development of novel therapeutics for *S. aureus* infections based on the *agr* quorum sensing system have predominately centered on the development of synthetic AIP analogs to directly compete with native AIP for AgrC binding. It has already been shown that cross-group antagonism of the *agr* response by heterologous AIPs can be used to attenuate the spread of infection in animal models (Mayville *et.al.*, 1999). More recently, synthetic AIPs with a minimized pharmacore have been created, however attempts to employ these as viable pharmaceutical inhibitors of *S. aureus* infection have been largely unsuccessful due to the presence of four distinct *agr* specificity groups, each with individual variations in AIP structure and AgrC sensor domain amino acids (George *et.al.*, 2008; Lyon *et.al.*, 2000).

The most exciting developments in chemical agents capable of blocking *S. aureus* autoinducer:receptor binding have been fostered predominantly within the past two years, marking the onset of era of significant discovery with regards to staphylococcal therapeutics. Park and colleagues reported the use of a complementary murine monoclonal antibody, AP4-24H11, capable of sequestering the *S. aureus agr* group IV strain AIP-4 from its cognate AgrC receptor (Park *et.al.*, 2007). In this manner AP4-2AH11 effectively "quenches" the QS response, increasing protein A expression and decreasing α-hemolysin and RNAIII transcription (Kirchdoerder *et.al.*, 2011; Tal-Gan *et.al.,* 2013). It has also been shown that *Lactobacillus reuteri* is capable of inhibiting staphylococcal *agr* quorum sensing through the cyclic dipeptides cyclo-(Tyr-Pro) and cylco-(Phen-Pro), predominantly employed during interspecies communication. This work highlights not only the possibility of bacterial cross-talk between distinct signaling systems, but also the potential use of human probiotic isolates in the inhibition of bacterial virulence, specifically staphylococcal species responsible for toxic shock syndrome (Li *et.al.*, 2011; Tal-Gan *et.al.*, 2013). Perhaps most recently, structure-activity relationship studies of the relatively uncharacterized *S. aureus* AIP-III has lead to the development of several AIP-III analogs that are capable of global inhibition of the *S. aureus agr* QS circuit, and represent the most potent inhibitors to date. Paramount, is the AIP-III analog AIP-III D4A, which surpassed the activity of the known inhibitor tAIP-I D2A by 5- to >20-fold in reporter assays. Other significant inhibitors were identified as having modifications in residues Ile1 and Asn2. Overall, this study suggests that AIP-III presents a superior scaffold for the development of QS peptide inhibitors, and represents a

strong chemical and biochemical basis for the optimization and analysis of these peptide-based inhibitors as *S. aureus* therapeutics (Tal-Gan *et.al.*, 2013).

While peptide therapeutics are not a new concept in the field of pharmaceuticals they have been largely unsuccessful due to cost, size constraints, short half-life and lack of adequate delivery methods, among others (Giuliani *et.al.*, 2011; Lu *et.al.*, 2006). More recently, however, advancements in peptidomimetic approaches and the isolation and manipulation of previously unavailable and highly toxic naturally occurring peptides, have brought peptide therapies back into the realm of viable pharmaceuticals. Aurein 1.2, for example, is a naturally occurring highly toxic peptide secreted from Australian Southern Bell Frogs, which has recently been isolated and shows active antibacterial action towards *Leuconostoc lactis*, *S. aureus*, and *Staphylococcus epidermis* (Pan *et.al.*, 2007). Protein epitope mimetics, multimeric peptides, synthetic lipidated peptides and peptoids are just some of methods explored thus far to improve peptidomimetics while maintaining the basic features of membrane-active natural antimicrobial peptides (Giuliani *et.al.*, 2011).

With the continual use of antibiotics to combat *S. aureus* infections and lack of novel therapeutic strategies, resistance to other classes of antibiotics and the emergence of novel multi-drug resistant strains of *S. aureus* will undoubtedly occur. *S. aureus* infections, specifically with regards to MRSA, are already considered an epidemic and with the acquisition of virulence cassettes and super antigens the disease states induced by this bacteria and severity of infection are bound to worsen.

1.6 Thesis Objectives

The fundamental objective of this work was to create successive truncations of the response regulator protein AgrA, and to identify if these truncations, when expressed intracellularly from a transformed plasmid, could block the staphylococcal quorum sensing response through inhibition of the ArgC:AgrA interaction.

Qualitative and quantitative hemolysis assays and qualitative real-time polymerase chain reaction (qRT-PCR) were used to assess the efficacy of aformentioned AgrA truncations as dominant negative inhibitors of *agr* quorum sensing. Additionally, Phos-tag™ gel electrophoresis technology was employed in the identification of truncation protein phosphorylation states, allowing for inference of AgrC:AgrA-truncation interactions.

1.7 Hypothesis

We hypothesize that AgrA truncations expressed in *S. aureus* by the staphylococcal shuttle vector pCN47 will be sufficient to inhibit the AgrC:AgrA interaction. Moreoever, we hypothesize that inhibition of this interaction by an AgrA truncation dominant negative inhibitor will effectively block quorum sensing and the downstream production of virulence genes, including the hemolysin toxins.

CHAPTER TWO

2.0 MATERIALS & METHODS

2.1 Microbiological Methods

2.1.1 Cultivation of *Escherichia coli*

E. coli XL-1 or BL21 (*DE3*) cells (Stratagene, La Jolla, CA, USA) were grown under aerobic conditions at 37°C in liquid Luria-Betani broth (LB; 1% (w/v) bacto-tryptone, 0.5% (w/v) bacto yeast extract, 1% (w/v) NaCl) with shaking at 250 rpm or on solid LB agar plates (1.5% w/v) supplemented with antibiotics. Antibiotics were used at 100 μg/mL for ampicillin or 30 μg/mL for kanamycin (Kan). Glycerol stocks of cultures for long-term storage were prepared by combining stationary phase liquid culture with glycerol to a final concentration of 20% (v/v). Stocks were flash frozen with liquid nitrogen at stored at -80°C.

2.1.2 Transformation of *E. coli*

For transformations, 1 μL (50-150 ng) of prepared plasmid DNA was added to 50 μL chemically competent *E. coli* XL-1 or BL21 (*DE3*) cells (Stratagene, La Jolla, CA, USA) and incubated on ice for 30 minutes. Cells were then heat shocked for 45 seconds in a 42°C water bath, and returned to ice for 2 minutes. A 250 μL aliquot of Super Optimal Broth with Catabolite Repression (SOC) medium (2% (w/v) bacto tryptone, 0.5% (w/v) yeast extract, 8.56mM NaCl. 2.5 mM KCl, 10mM $MgCl_2$, 20 mM $MgSO_4$, and 20 mM glucose) was added to heat shocked cells. Cells were grown at 37°C for 1 hour with shaking at 250 rpm, followed by plating on pre-warmed LB agar plates

containing appropriate antibiotic. Plates were incubated overnight at 37°C to allow for colony growth.

2.1.3 Cultivation of *S. aureus*

S. aureus agr$^+$ laboratory wild type strain RN6734 (Richard P. Novick, New York University, New York, NY, USA) or the cloning intermediate RN4220 (Roger Plaut, Food & Drug Administration, Bethesda, MD, USA) were grown under aerobic conditions at 37°C in tryptic soy broth (TSB; Becton, Dickinson & Co., Oakville, ON, CAN; 1.7% (w/v) pancreatic digest of casein, 0.3% (w/v) papaic digest of soybean meal, 0.5% (w/v) NaCl, 0.25% K_2HPO_4, 0.25% glucose) with shaking at 250 rpm or on solid TSB agar plates (1.5% w/v). Glycerol stocks of cultures for long-term storage were prepared by combining stationary phase liquid culture with glycerol to a final concentration of 20% (v/v). Stocks were flash frozen with liquid nitrogen at stored at -80°C.

2.1.4 Electrocompetent *S. aureus* Cells

Overnight cultures of *S. aureus* RN4220 or RN6734 grown in B2 broth (1% (w/v) casein hydrolysate, 2.5% (w/v) yeast extract, 0.1% (w/v) K_2HPO_4. 0.5% (w/v) glucose, 2.5% (w/v) NaCl) with constant aeration at 37°C were diluted 1:25 in fresh B2 broth. Cells were grown under aerobic conditions at 37°C with shaking at 250 rpm, until an OD_{600} of 0.4 was reached. Cells were then harvested by centrifugation at 4000 rpm. Upon harvesting, cells were washed three times in an equal volume of deionized water, followed by second washes in 10% (v/v) glycerol. Following resuspension in the second

10% (v/v) glycerol solution, the cell suspension was incubated for 15 minutes, centrifuged at 40000 rpm and the pellet was resuspended in 800 μL of 10% (v/v) glycerol. Aliquots of electrompetent cells were stored at -80°C immediately after preparation.

2.1.5 Electroporation of *S. aureus* Cells

Frozen competent cells were thawed on ice for 30 minutes prior to addition of 1 μg of prepared plasmid DNA. The suspension was incubated an additional 30 minutes on ice, then transferred to 0.1 cm gap Gene Pulser electroporation cuvettes (Bio-Rad, Mississauga, ON, CAN). The cell-DNA suspension was electroporated at 100 Ohms (Ω), 25uF capacitance, and 2.3kV in a Bio-Rad Gene Pulser II. Electroporated cell suspensions were immediately placed on ice and resuspended in 940 μL B2 broth. The cell suspensions were transferred to eppendorf microcentrifuge tubes, previously on ice, and incubated at 37°C for at least 2 hours. Suspensions were plated on tryptic soy agar (TSA) with 5 μg/ml erythromycin (Erm), and incubated at 37°C for 48 hours.

2.1.6 Staphylococcal DNA Extraction

S. aureus RN6743 genomic DNA was isolated using the NucliSENS MiniMag extraction kit (BioMerieux, Marcy l'Etoile, France) from staphylococcal overnight cultures grown in TSB. *S. aureus* culture was diluted 1:10 in lysis buffer and incubated at room temperature for 10 minutes, then briefly vortexed for 10 seconds. Silica was added, followed by sample vortexing and a second 10 minute incubation at room temperature. The specimen was then centrifuged for 2 minutes at 2000 rpm in a Beckman GPR Benchtop centrifuge, followed by resuspension in 400 μL Wash Buffer 1. The

resuspended pellet was then washed for 30 seconds on the MiniMag (BioMerieux). Samples were washed, as described above, a total of twice with Wash Buffer 1, followed by two washes with 500 μL Wash Buffer 2, and two washes with 500μ Wash Buffer 3. Upon completion of wash steps, 50 μL elution buffer was added and samples were centrifuged 5 minutes at 1400 rpm and 60°C on the Thermomixer 5436 Eppendorf centrifuge (Capital Scientific Inc., Austin, TX, USA). Eluted DNA was stored a -20°C.

2.2 Molecular Biological Methods

2.2.1 Gateway Cloning Procedures and Plasmids

Constructs were amplified from *S. aureus* RN6734 using Platinum® Pfx DNA polymerase (Invitrogen; Life Technologies Inc., Burlington, ON, CAN). All gene specific primers were synthesized by Sigma-Aldrich Corporation (Oakville, ON, CAN) and contained the *attB*- recombination sites. Oligonucleotide primer sequences are listed in Appendix 6.2.

Purified PCR products were cloned into the $pDONR_{201}$ vector (Gateway®; Invitrogen) using the *attB*-sites of the PCR product, incorporated via primers with the 5' Gateway sequences, and the *attP*-sites on the donor vector. Prepared PCR product (150 ng) was incubated with the $pDONR_{201}$ donor vector (150 ng) and BP clonase® II enzyme mix (Integrase, Integration Host Factors; Gateway®, Invitrogen) and incubated for 1 hour at room temperature. The reaction was stopped with the addition of Proteinase K (0.2 μg/mL; Gateway®, Invitrogen) and incubation at 37°C for 10 minutes. The resulting entry vectors (*pENT*) contain kanamycin (kan) resistance and the gene of interest flanked by *attP*-sites. Entry vectors were transformed into *E. coli* XL-1 cells (Stratagene) followed by plating on LB agar plates containing 30 μg/mL kanamycin for antibiotic selection of $pDONR_{201}$. Plates were incubated at 37°C overnight. Single colonies were picked from the plates and added to LB supplemented with 30 μg/mL kanamycin, and grown overnight at 37°C with shaking at 250 rpm. Plasmids were extracted from cultures and purified using the GenElute Plasmid Miniprep kit (Sigma-Aldrich).

To generate exit (*pEX*) vectors containing ampicillin antibiotic resistance and the gene of interest flanked by *atttR*-sites, the purified entry vector (150 ng) was incubated with either the $pDEST_{15}$ or $pDEST_{17}$ vector (150 ng), containing a N-terminal glutathione-

S-transferase (GST) and His_6 eptiope tag respectively, and LR clonase® II enzyme mix (Integrase, Exisionase, Integration Host Factors; Gateway®, Invitrogen). The reaction proceeded for 1 hour at room temperature and was stopped by the addition of Proteinase K (0.2 μg/mL; Invitrogen) and a 10 minute incubation at 37°C. Exit vectors were transformed into *E. coli* XL-1 cells (Stratagene) followed by plating on LB agar plates containing 100 μg/mL ampicillin. Plates were incubated at 37°C overnight. Single colonies were picked from the plates and added to LB supplemented with 100 μg/mL ampicillin, and grown overnight at 37°C with shaking at 250 rpm. Plasmids were extracted from cultures and purified using the GenElute Plasmid Miniprep kit (Sigma-Aldrich). All constructs were verified by sequencing at the Institute for Molecular Biology and Biotechnology (MOBIX; McMaster Univeristy, Hamilton, ON, CAN). Plasmids and strains are listed in Appendix 6.3.

2.2.2 Traditional Cloning Procedures and Plasmids

Constructs were amplified from *S. aureus* RN6734 using Platinum® Pfx DNA polymerase (Invitrogen; Life Technologies Inc., Burlington, ON, CAN). All gene specific primers were synthesized by Sigma-Aldrich Corporation (Oakville, ON, CAN) and contained a 5' His_6 epitope tag, in addition to either a 5' BamHI or 3' EcoRI restriction sequence. Oligonucleotide primer sequences are listed in Appendix 6.2.

Purified PCR products were cloned into the multiple cloning site (MCS) of the staphylococcal vector pCN47 (Patrick Linder, University of Geneva, Geneva, Switzerland). Briefly, PCR products (1 μg) and the vector pCN47 (1 μg) were incubated with 10 units of the high fidelity (HF) restriction enzymes EcoRI-HF and BamHI-HF

(New England BioLabs, Ipswich, Massachusetts, USA) in 1X NEBuffer 4 for 1 hour at 37°C. Products were PCR purified and vector pCN47 was subjected to phosphatase treatment to prevent vector relegation. A 1:10 volume of 10X Antarctic Phosphatase Reaction Buffer was added to 1-5 μg of restriction digested vector DNA, followed by the addition of 1μL of Antarctic Phosphatase (5 units; New England BioLabs). The reaction was incubated at 37°C for 1 hour and heat inactivated at 70°C for 5 minutes.

Restriction digested PCR products were ligated into restriction enzyme and phosphatase treated vector pCN47. A 3-fold or 10-fold molar mass of PCR product insert was combined with 50 ng of vector, 1X T4 DNA Ligase Buffer, and 1 μL of T4 DNA Ligase. The volume was adjusted to 10 μL and the reaction was incubated at 16°C for 16 hours. All constructs were verified by sequencing at the Institute for Molecular Biology and Biotechnology (MOBIX). Plasmids and strains are listed in Appendix 6.3.

All constructs were transformed into the cloning intermediate strain RN4220 (Roger Plaut) and extracted from cultures and purified using the GenElute Plasmid Miniprep kit (Sigma-Aldrich). Purified plasmids were then transformed into RN6734 (Richard P. Novick) for expression.

2.2.3 Quantitative Real Time PCR (qRT-PCR)

RNA was extracted from *S. aureus* RN6734 strains using the Qiagen RNeasy® Mini-Kit (Mississauga, ON, CAN). All gene specific primers and probes were synthesized by Biosearch Technologies Inc (Novato, CA, USA). Oligonucleotide primer sequences are listed in Appendix 6.2.

RNA was extracted from RN6734 transformed with vector pCN47 constructs as per the RNeasy® Mini-Kit instructions, with extra care taken to maintain an RNase free environment. Following extraction, RNA was treated with DNase I (Invitrogen) in a reaction that contained 1 μg RNA, 1 μL DNase I (2 units) and 1X DNase I Reaction Buffer to a final volume of 10 μL. The reaction was incubated at 37°C for 30 minutes and stopped by the addition of 1 μL 25 mM EDTA with heat inactivation at 65°C for 10 minutes.

DNase treated RNA products were then subjected to reverse transcription by M-MLV Reverse Transcriptase (Invitrogen). Briefly, 5 μL of DNase treated RNA was combined with 7 μL of dNTP Buffer (57% (v/v) 2.5 mM dNTP, 13% (v/v) random primers, dH_2O to 7 μL). The reaction was heated for 5 minutes at 70°C, and chilled on ice until samples had cooled. To the reaction mixture, 7 μL of FS Buffer (57% (v/v) 5X 1st Strand Buffer, 13% (v/v) 0.1 M DTT, 30% (v/v) Invitrogen RNaseOut (40 units/μL) was added and the reaction was heated at 37°C for 2 minutes. To each of the samples, 1 μL of M-MLV reverse transcriptase was added, followed by incubation at room temperature for 10 minutes. The reaction was incubated a final time at 37°C for 50 minutes and the reaction was stopped by heat inactivation at 70°C for 15 minutes. cDNA samples were stored at -20°C until further use.

Two step real time PCR (qRT-PCR) was performed using the QuantiTect® Probe PCR kit (Qiagen). A 25 μL/reaction master mix was prepared containing 1X QuanitTect Probe PCR Master Mix, 0.4 μM *hla* forward primer, 0.4 μM *hla* reverse primer, 0.2 μM *hla*-specific probe, 5 μL complementary DNA (cDNA) and RNase-free water. Prepared samples were placed into the Rotor-Gene Q real-time cycler (Qiagen), which was

programed with a 15 minute PCR initial activation step at 95°C, followed by 2-step cycling. The 2-step cycling was comprised of a 15 second denaturuation at 94°C followed by a combined annealing/extension step for 60 seconds at 60°C. The real-time cycler was set to complete 40 cycles, after which data analysis was performed.

2.2.4 Production of Soluble Recombinant Protein in *E. coli*

All constructs were expressed in *E. coli* BL21 (*DE3*) cells (Stratagene). Expression plasmids transformed in BL21 (*DE3*) were plated on LB agar plates containing 100 μg/mL ampicillin. LB broth, containing 100 μg/mL ampicillin, was then inoculated with a 1:50 dilution of overnight culture and grown at 37°C with shaking at 250 rpm until a optical density of approximately 0.6 at 600nm (OD_{600}) was reached. Cultures were induced with 0.1 M of isopropyl- -thiogalactopyranoside (IPTG; Sigma-Aldrich) and incubated for 2 hours at 37°C with shaking at 250 rpm. Bacteria were harvested by centrifugation at 7000 rpm in a Sorvall GSA rotor for 5 minutes at 4°C in a Sorvall RC-5B centrifuge. The resulting bacterial pellet was resuspended in 10 mL of ice cold Nickel A Buffer (20 mM ris-HCl pH 7.2, 500 mM KCl, 10 mM imidazole, 10% (v/v) glycerol, 0.2% (v/v) -mercaptoethanol (-ME), 0.03% (v/v) lauryldimethylamine-oxide (LDAO)) for purification on nickel-NTA agarose.

2.2.5 Production of Soluble Recombiant Protein in *S. aureus*

All constructs were expressed in *S. aureus* RN6734 cells (Richard P. Novick). Expression plasmids transformed into *S. aureus* RN6734 were plated on TSA plates containing 5 μg/mL erythromycin. TSB containing 5 μg/mL erythromycin, was

inoculated with a 1:50 dilution of overnight culture and grown at 37°C with shaking at 250 rpm until an optical density of approximately 0.5 at 595nm (OD_{595}) was reached. Bacteria were harvested by centrifugation at 7000 rpm in a Sorvall GSA rotor for 5 minutes at 4°C in a Sorvall RC-5B centrifuge. The resulting bacterial pellet was resuspended in 10 mL of ice ice cold Nickel A buffer (20 mM ris-HCl pH 7.2, 500 mM KCl, 10 mM imidazole, 10% v/v glycerol, 0.2% (v/v) -mercaptoethanol (-ME), 0.03% (v/v) LDAO) for purification on nickel-NTA agarose.

2.2.6 Purification of Recombinant Protein

Culture suspensions were sonicated on ice using the Fisher Sonic Dismembrator Model 100 (Fisher Scientific, Ottawa, ON, CAN). The lysates were centrifuged at 18,500 rpm in a Sorval GSA rotor for 45 minutes at 4°C in a Sorvall RC-5B centrifuge to remove insoluble material. Supernatants were filtered through 0.45 μm acrodisc filters (Pall Corporation, Port Washington, NY, USA). The lysate was then loaded into a Superloop colum (GE Healthcare, Mississauga, ON, CAN) and purified via affinity chromatography on the Akta FPLC (Amersham Bioscience, Uppsala, Sweden). Protein lysates were bound to a His-Trap™ HP Column (GE Healthcare) and washed with Nickel A buffer 20 mM ris-HCl pH 7.0, 500 mM KCl, 10 mM imidazole, 10% (v/v) glycerol, 0.03% (v/v) LDAO). Columns were washed with increasing concentrations of imidazole, and bound protein was eluted off the column in pure Nickel B buffer (20 mM Tris-HCl pH7.0, 500 mM KCl, 300 mM imidazole, 10% (v/v) glycerol, 0.03% (v/v) LDAO). Eluted protein was dialyzed against phosphate buffered saline (PBS) + 10% (v/v) glycerol, followed by quantification through comparison to BSA standards. Purity was confirmed using sodium

dodecyl sulfate polyacrylamide gel electrophoresis (SDS-PAGE) and Coomassie blue staining (45% (v/v) methanol, dH_2O, 10% (v/v) acetic acid, 0.25% (w/v) R-250 Brilliant Blue).

2.2.7 *In vitro* Kinase Assay

Endogenous AgrA proteins contain an aspartate phophoacceptor residue that becomes phosphorylated by phosphortransfer from activated AgrC at the onset of quorum sensing. Engineered AgrA truncations, expressed in the laboratory *agr*$^+$ strain RN6734, were designed with the maintenance of this phosphoacceptor site. To determine the phosphorylation state of the truncations, cultures of RN6734 strains expressing AgrA truncations were grown at 37°C with shaking at 250 rpm overnight. Cultures were centrifuged at 3000 rpm for 5 minutes, and the supernatant was discarded. Remaining bacterial pellets were resuspended in 5X sample buffer (250 mM Tris pH 6.8, 12.5% (v/v) -ME, 32.3% (v/v) glycerol, 6.25% (v/v) SDS, 0.001% (w/v) bromophenol blue), and boiled for 5 minutes. Prepared samples were then run on a Phos-tag™ gel in conjunction with phosphatase treated controls, as described below.

2.2.8 *In vitro* Phosphatase Assay

Antarctic Phosphatase was used to dephosphorylate recombinant protein for use as a control in Phos-tag™ experiments. Briefly, RN6734 transformed with pCN47 recombinant vectors was grown overnight in 1X TSB containing 5 μg/mL erythromycin at 37°C with shaking at 250 rpm. Cultures were sonicated for 10 seconds to lyse cellular membranes, followed by centrifugation at 3000 rpm for 10 minutes to pellet cellular

debris and unbroken cells. The resulting supernatant (10 µL) was combined with a 1:10 volume of 10X Antarctic Phosphatase Reaction Buffer, 1µL or Antarctic Phosphatase (5 units; New England BioLabs), and water to 50 µL. The reaction was incubated at 37°C for 1 hour. Protein samples were resuspended in 3X sample buffer and loaded on a Phos-tag™ acrylamide gel for detection.

2.2.9 NLS-AgrA$_{1-64}$ Cellular Uptake Assay

To determine if a nuclear localization signal (NLS) would be able to facilitate cellular uptake of His-maltose binding protein (MBP)-NLS-AgrA$_{1-64}$ into *S. aureus* RN6734 cells 4 mL of overnight RN6734 was harvested by centrifugation at 8000 x *g* for 2 minutes. The supernatant was discarded and 100 µL of 100 µM His-MBP-NLS-AgrA$_{1-64}$ peptide solution in LB was added, followed by resuspension of the cells. The peptide mixture was incubated at 37°C for 1 hour, followed by a second centrifugation at 8000 x *g* for 2 minutes to harvest the cells. A 400 µL aliquot of the supernatant was retained to which 40 µL of 2X sample buffer was added, followed by boiling at 95° for 5 minutes. The cells were washed twice with PBS and resuspended in 30 µL od 2X sample buffer. For a proteinase K control 2 µL of 20 mg/mL proteinase K was added to the solution and incubated at 37° for 10 minutes.

2.2.10 Phos-tag™ SDS-PAGE

To a standard SDS-PAGE resolving gel solution (30% (v/v) acrylamide:bis (Bio-Rad), 8X resolving gel buffer (3 M Tris-HCl pH 8.8, 0.8% (v/v) SDS), dH_2O, 20% (v/v)

SDS, 0.15% (w/v) ammonium persulfate (APS), 0.004% (v/v)tetramethlethylenediamine (TEMED)), 42 μL of both Phos-tag™ acrylamide and 10 mM $McCl_2$ were added. The Phos-tag™ resolving gel solution was used to cast 12% (v/v) acrylamide gels, followed by a standard stacking gel solution (30% (v/v) acrylamide:bis (Bio-Rad), 4X stacking gel buffer (0.4 M Tris-HCl pH 6.8, 0.8% (v/v) SDS), dH_2O, 20% (v/v) SDS, 0.15% (w/v) APS, 0.004& (v/v) TEMED). Protein samples were resuspended in 5X SDS-PAGE loading buffer (250 mM Tris pH 6.8, 12.5% (v/v) -ME, 32.3% (v/v) glycerol, 6.25% (v/v) SDS, 0.001% (w/v) bromophenol blue), heated for 5 minutes at 95°C and loaded onto a prepared Phos-tag™ gel. The gel was electrophoresed for 20 minutes at 80 V to allow protein movement throughout the stacking gel, followed by electrophoresis at 120 V for 80 minutes until the dye front reaches the bottom of the resolving gel. Prior to transfer of the proteins to a nitrocellulose membrane, the Phos-tag™ acrylamide gels were soaked in 10 mM ethylenediaminetetraacetic acid (EDTA)- transfer buffer and EDTA-free transfer buffer (1.44% (w/v) glycine, 0.3% (w/v) Tris, 10% (v/v) methanol, dH_2O). Gels were transferred to a nitrocellulose membrane using the iBlot Gel Transfer apparatus (Invitrogen) at 25 V for 10 minutes. Western blot detection of His_6-tagged proteins proceeded as described below.

2.2.11 Western Blot Analysis

Protein samples were resuspended in 5X SDS-PAGE loading buffer (250 mM Tris pH 6.8, 12.5% (v/v) -ME, 32.3% (v/v) glycerol, 6.25% (v/v) SDS, 0.001% (w/v) bromophenol blue), heated for 5 minutes at 95°C and loaded on a 12% SDS-PAGE gel. The gel was electrophoresed for 20 minutes at 80 V to allow protein movement

throughout the stacking gel, followed by electrophoresis at 120 V for 80 minutes until the dye front reaches the bottom of the resolving gel. Proteins were transferred from the agarose gel to a nitrocellulose membrane using the iBlot® Gel Transfer apparatus (Invitrogen) at 20 V for 7 minutes. Membranes were blocked with 5% skim milk powder in PBS + 0.1% Tween-20 for 1 hour at room temperature. Polyclonal mouse anti-His_6 antibody diluted 1:5000 in 5% skim milk powder and 20 mL PBS + 0.1% Tween-20 was incubated with blocked membranes for 1 hour at room temperature. Membranes were washed twice for 5 minutes with PBS + 0.1% Tween-20 prior to probing with a polyclonal goat anti-mouse IgG antibody diluted 1:5000 in 5% skim milk power and 20 mL PBS + 0.1% Tween-20. Incubation occurred for 1 hour at room temperature. Membranes were washed as described previously. Blots were visualized using enhanced chemiluminescence (ECL) substrates (Sigma-Aldrich) and CL-X Posture™ film (Thermo Scientific, Waltham, MA, USA) and developed in a Konica Minolta medical X-ray processor.

2.2.12 *In vitro* Hemolysis Assay

Overnight cultures of RN6734 strains were diluted 1:100 in fresh TSB media with 5 μg/mL erythromycin. AIP-III D4A (Helen E. Blackwell; University of Wisconsin-Madison, Madison, WI, USA) 10 μM stock solutions were diluted with DMSO in serial dilutions (1:3 or 1:5), and 2 μL of the peptide solution was added to the wells of a clear 96-well microtitre plate (Sarstedt; Newton, NC, USA). A 198 μL portion of RN6734 diluted culture was added to each of the peptide-containing wells. A 198 μL portion of diluted transformed RN6734 strains (RN6734-pAR1, RN6734-pAR2, and RN6734-

pAR3) were added to separate empty wells of the microtitre plate. Plates were incubated statically at 37°C for 6 hours, and the cultures were then assayed for hemolytic activity. Suspended red blood cells (5 mL) were raised to 14 mL with sterile saline phosphate buffer (PBS; pH= 7.35, 9 mL) and centrifuged (2500 rpm, 25C, 5 minutes). The supernatant was removed and resuspension and centrifugation were repeated three times. A 13 μL portion of the suspended red blood cells was added to each well. The microtitre plate was incubated statically at 37°C for 15 minutes, followed by centrifugation to pellet the cells (450 *g*, 4 minutes, 25°C). A 150 μL aliquot of supernatant from each well was transferred to a fresh microtitre plate and absorbance at 420 nm was measured for each well using a plate reader (μQuant; Biotek Instruments Inc, Winooski, VT, USA). Percent lysis was calculated as follows:

$$\frac{value-background}{lysis-background}\ X\ 100$$

Conversely, percent inhibition was calculated as follows:

$$\frac{RN6734\ activity-inhibited\ activity}{RN6734\ activity}\ X\ 100$$

For qualitative analysis of hemolysis using TSB with 5% sheep blood agar plates, overnight cultures of RN6734 strains, RN4220 and RN9688 were spotted in 10 μL aliquots. Plates were incubated at 37°C for 48 hours to allow for the production of hemolysins.

CHAPTER THREE

3.0 RESULTS

3.1 Construction of AgrA Truncations

Previous attempts to express and crystallize full-length constructs of *S. aureus* AgrA have been largely unsuccessful, however to date no biochemical explanation has been put forth to explain this phenomenon. Moreover, AgrA crystallization attempts were only made possible by the truncation of AgrA, and subsequent co-crystallization with its DNA target. AgrA contains two major domains, each with highly specific functions. The N-terminal receiver REC domain contains intermolecular interaction sites, a dimerization domain, and the highly conserved aspartate phosphoacceptor that is responsible for coordinating an incoming phosphate residue transferred from the cognate histidine kinase. The C-terminal CheY-like LytTR domain facilitates DNA binding, and subsequent downstream signaling that is regulated by response regulator AgrA.

With knowledge of the limitations of AgrA expression, and based on previously established domain boundaries, an initial protein truncation encompassing the entire REC domain was created. The resulting $AgrA_{1\text{-}136}$ protein was then further truncated, with emphasis on maintaining the putative phosphoacceptor site at aspartate 59 (D59). Retaining this residue in all constructs permitted downstream phosphorylation analysis, providing further indication of the efficacy of the truncation proteins to disrupt quorum sensing. Truncations $AgrA_{1\text{-}136}$, $AgrA_{1\text{-}100}$, and $ArgA_{1\text{-}64}$ were created (Figure 3.1) and subsequently cloned into a *S. aureus* expression vector, pCN47, for eventual transformation into the staphylococcal *agr*-I strain RN6734. All constructs were engineered with a His_6-epitope tag to permit Western blot detection.

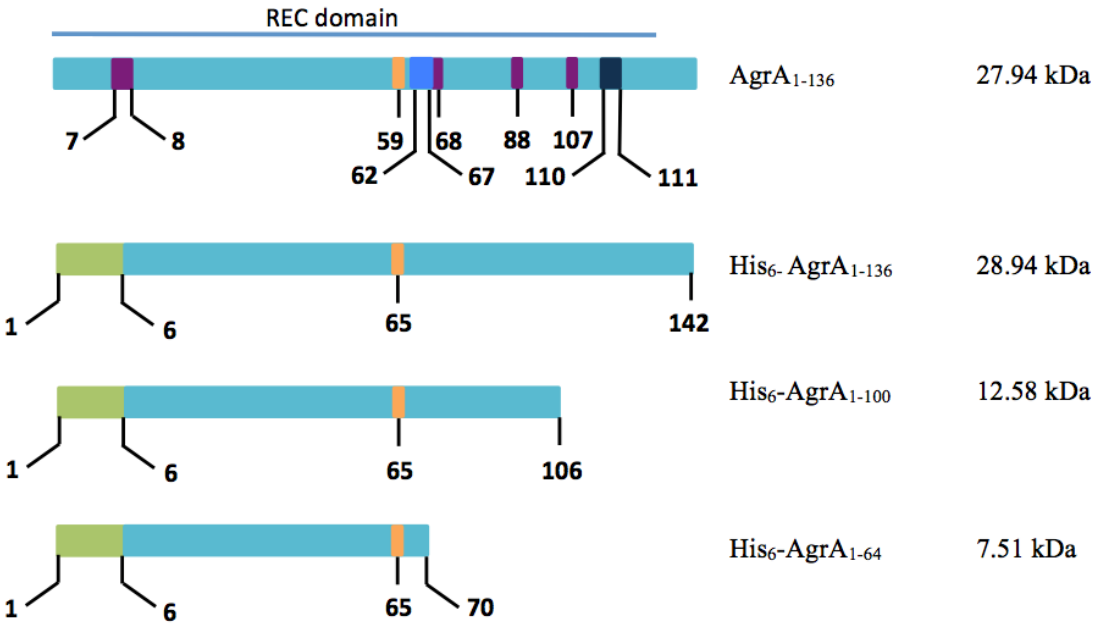

Figure 3.1 Schematic diagram of $AgrA_{1-136}$ conserved domains and the created AgrA truncations. Full length AgrA is not soluble, and thus the protein must be expressed as a truncation of the full-length 238 amino acid protein. The N-terminal domain of AgrA, $AgrA_{1-136}$ is thought to encompass the well-conserved receiver REC domain, with C-terminal portions of AgrA mediating DNA-binding via a conserved LytTR domain. Three constructs, $AgrA_{1-136}$, $AgrA_{1-100}$, and $ArgA_{1-64}$, containing an N-terminal His_6 epitope were created as described in the methods section. The numbers underneath each diagram indicate relative amino acid location and constructs are shown from the amino to carboxy terminus (left to right). N-terminal His_6 tag is green, putative phosphorylation site is orange, hypothesized activation sites are purple, intermolecular recognition site is royal blue, and the dimerization interface is indigo. All domain locations are relative and were determined using the conserved domain function within BLAST (National Centre for Biotechnology Information; Bethesda, MD, USA). Molecular weight values are an estimation based on amino acid sequence and constructs are not to scale.

3.2 *S. aureus* RN6734 Strains Transformed with Expression Plasmids Exhibit a Decrease in Hemolytic Activity

3.2.1 AgrA Truncation Inhibit RN6734 Hemolysis on Sheep's Blood Agar Plates

In order to determine the effect of a dominant negative AgrA peptide mimetic on quorum sensing, previously constructed AgrA truncations inserted into the staphylococcal shuttle vector pCN47 (Table 6.3.2, Appendix) were transformed into the *agr*-I laboratory strain RN6734. Under normal conditions, activation of the *agr* quorum sensing autoactivation circuit by endogenous AIP molecules results in the production of both -and -hemolysins causing red blood cell lysis, as seen in Figure 3.2. RN6734 strains transformed with expression vector constructs (Table 6.3.1, Appendix) and staphylococcal controls were spotted onto TSA plates containing 5% sheep blood. The cloning intermediate RN4220, which predominately expresses -hemolysin, displays a partially turbid zone of clearing. RN9688, a *lux*-expression strain, shows no hemolysis indicative of the replacement of RNAIII with the *lux* operon. This reporter strain is a positive control, indicating what would be expected from complete inhibition of quorum sensing. Strains RN6734-pAR1 #1 and #2, RN6734-pAR2 and RN6734-pAR3 #1 and #2, expressing the truncations $AgrA_{1-136}$, $AgrA_{1-100}$ and $ArgA_{1-64}$ respectively, all display a marked decrease in hemolytic activity when compared to the wild-type RN6734 control (Figure 3.2).

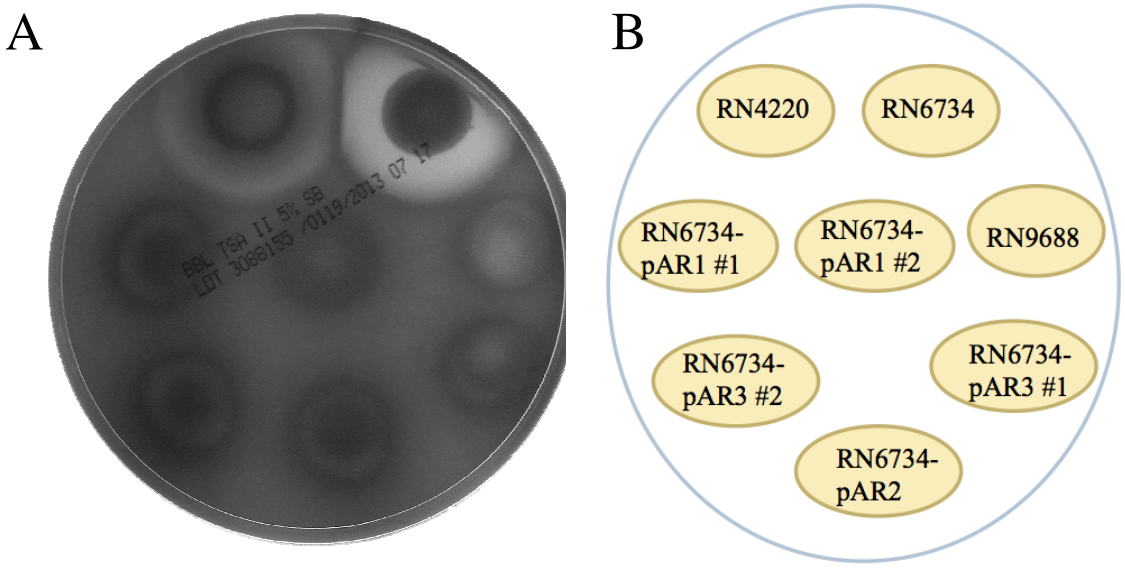

Figure 3.2: Transformation strains of RN6734 inhibit hemolysis when compared to untransformed controls. Transformed strains of RN6734 containing the pAR1, pAR2 or pAR3 expression plasmids, producing $AgrA_{1-136}$, $AgrA_{1-100}$ and $AgrA_{1-64}$ respectively, were grown overnight and spotted onto TSA with 5% sheep blood. **A.** The cloning intermediate RN4220 produces a partially turbid zone of clearing, indicative of -hemolysin production. Unlike RN6734, RN4220 does not produce -hemolysin and less effective as a hemolytic as a result. RN6734, an - and -hemolsyin producing strain displays a prominent zone of clearing, as is used as a hemolysis positive control. RN9688 is unable to produce hemolysins due to the replacement of the RNAIIII master regulator with the lux-operon. RN6734 pAR1 variants, RN6734-pAR2, and RN6734-pAR3 variants display no visible zones of clearing, indicating a reduction in hemolysis activity. **B.** Schematic diagram indicating the relative locations of the *S. aureus* cultures on the agar plate.

3.2.2 AgrA Truncations Inhibit RN6734 Hemolysis in an *in vitro* Hemolysis Assay

To quantify the qualitative results viewed in Figure 3.2, RN6734 strains were subjected to a microplate hemolysis assay. As a positive control, results were also compared to varying concentrations of the known quorum sensing inhibitor AIP-III D4A. Statistical significance was determined by comparing percent lysis of test samples to the RN6734 control, and was calculated using Student's unpaired t-test. Lysis buffer served as a negative control, and exhibited complete lysis of red blood cells, as seen in Figure 3.3. AIP-III D4A at a 5 μM concentration displayed the lowest hemolysis of all samples at 0.815 ± 1.41, and was statistically significant with a p-value of 0.0024. An increase in levels of hemolytic activity was seen for decreasing concentrations of AIP-III D4A at 1 μM, 0.1 μM, 0.033 μM and 0.02 μM, giving percent lysis values of 3.673 ± 6.362, 11.824 ± 17.33227, 15.406 ± 9.791 and 20.163 ± 14.210 respectively. Of these, only 1 μM AIP-III D4A and 0.033 μM AIP-III D4A were considered to be statistically significant reductions in hemolysis activity, with p-values of 0.0059 and 0.0375 respectively. RN6734-pAR3 variant 1, expressing the $AgrA_{1-64}$ truncation, displayed the most significant reduction in hemolytic activity of all the RN6734 transformation strains with a percent lysis of 2.293 ± 3.972, and was statistically significant with a p-value of 0.0036. Significant reductions in hemolysis were also evident in RN6734-pAR3 variant 2 with a percent lysis value of 9.228 ± 1.067, RN6734-pAR1 variant 1 expressing the $AgrA_{1-136-}$ truncation with a percent lysis value of 22.323 ± 1.854, and RN6734-pAR2 expressing the $AgrA_{1-100}$ truncation with a percent lysis value of 19.177 ± 6.684. The RN6734-pAR1 variant 2 strain did not exhibit a significant reduction in hemolytic activity with a percent lysis value of 21.744 ± 6.370, where the p-value equals 0.0546.

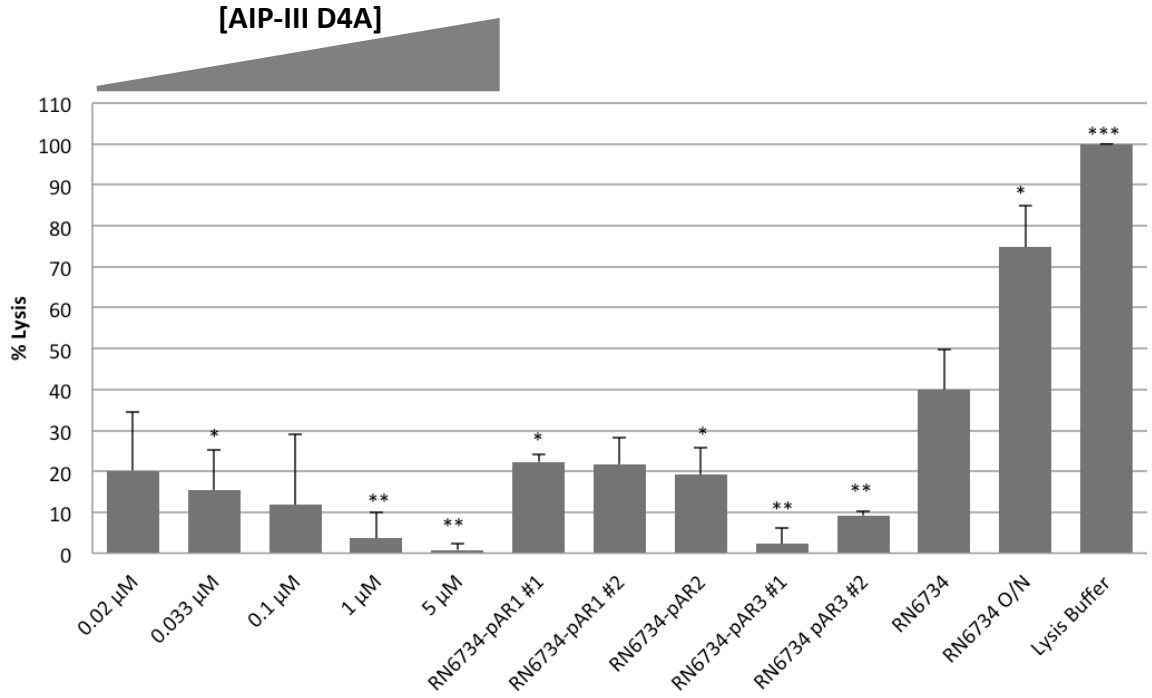

Figure 3.3: RN6734 transformed strains and the quorum sensing inhibitor AIP-III D4A exhibit a reduction in hemolysis when compared to the untransformed control. A. The quorum sensing inhibitor, AIP-III D4A, exhibits a significant reduction in hemolysis at concentrations of 0.033 µM, 1 µM and 5µM when compared to the RN6734 control. Strains RN6734-pAR1 variant #1, RN6734-pAR2, and RN6734-pAR3 variants #1 and #2 displayed a significant decrease in hemolytic activity as compared to untransformed RN6734. Overnight cultures of RN6734, that were not diluted 1:100, displayed an increase in percent lysis. The lysis buffer is a control indicative of complete lysis. Statistical significance was determined using the Student unpaired t-test to generate p-values; * significant at $p < 0.05$, ** significant at $p < 0.01$, *** significant at $p < 0.001$.

3.2.3 AgrA Truncations Exhibit up to 94% Inhibition of RN6734 Hemolysis

To further demonstrate the reduction in hemolytic activity displayed by the quorum sensing inhibitor AIP-III D4A, as well as the engineered RN6734 AgrA-truncation expressing strains, percent lysis values obtain from the microplate hemolysis assay were converted into values of percent inhibition, as seen in Figure 3.4. Trends seen for percent lysis in Figure 3.3 are inversely proportional to those for percent inhibition. A 5 μM concentration of AIP-III D4A displayed the greatest inhibition of hemolysis with a percent inhibition value of 97.963 ± 3.528. The capacity of AIP-III D4A to inhibit hemolytic activity of RN6734 decreased with a reduction in peptide concentration. AIP-III D4A concentrations of 1 μM, 0.1 μM, 0.033 μM and 0.02 μM inhibited hemolysis by 90.817% ± 15.905, 70.442% ± 43.327, 61.487% ± 24.475 and 49.597% ±35.523 respectively. Of the engineered staphylococcal strains, RN6734-pAR3 variant 1 exhibited the greatest inhibition of hemolysis at 94.268% ± 9.928. RN6734-pAR3 variant 2, inhibited hemolysis by 76.931% ± 2.667, and thus was the second most effective quorum sensing inhibitor of the AgrA truncations. RN6734-pAR1 variants 1 and 2 inhibited hemolysis by 44.196% ± 35.523 and 45.646% ± 15.924 respectively, while RN6734-pAR2 displayed a 52.061% ± 16.709 reduction in the hemolytic activity of RN6734. The aforementioned three constructs were less effective as quorum sensing inhibitors than the lowest concentration of AIP-III D4A, at 0.02 μM.

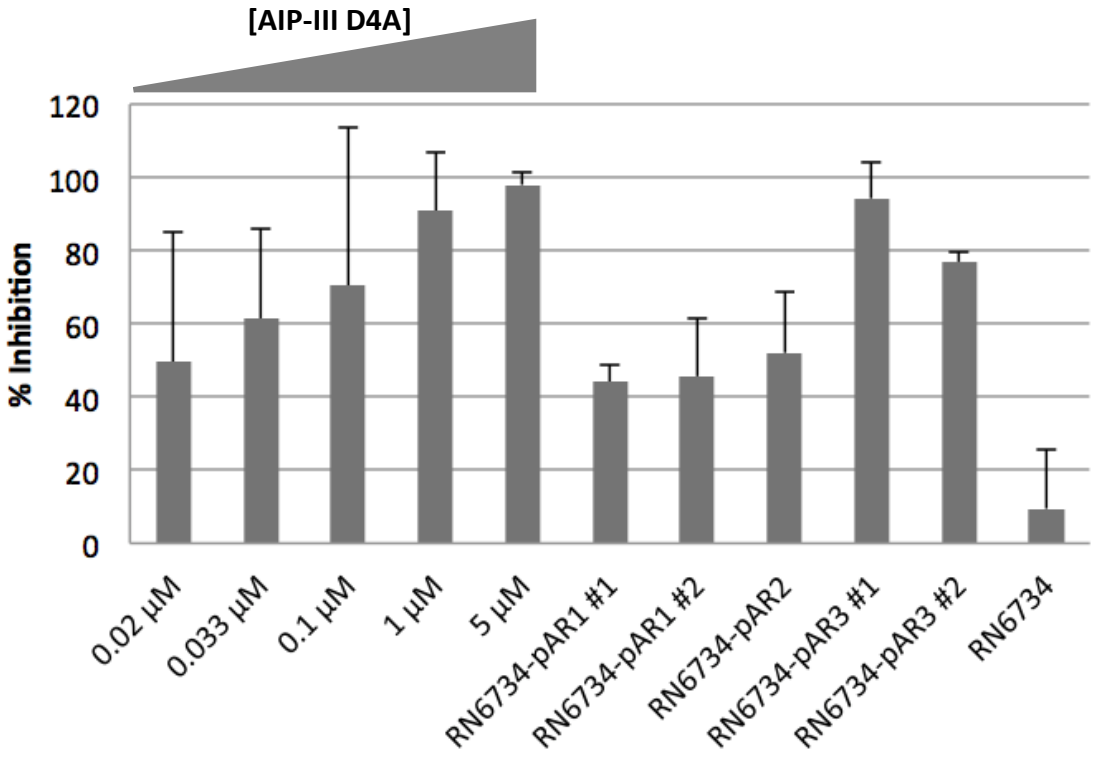

Figure 3.4: RN6734 transformed strains and the quorum sensing inhibitor AIP-III D4A display greater than 40% inhibition of quorum sensing when compared to the untransformed control. Percent inhibition of quorum sensing, as a function of reduction in hemolysis, was determined for each sample tested. Values of percent inhibition were calculated using RN6734 as a control. Of all the samples tested a 5 µM concentration of AIP-III D4A was most effective, with approximately 98% inhibition, followed closely by RN6734-pAR3 #1 with approximately 95% inhibition. Error bars represent 2 standard errors from the mean.

3.3 AgrA Truncation Constructs are Phosphorylated *in vitro*

AgrA truncations were designed with maintenance of the predominate phosphoacceptor, aspartate 59, in mind. As such, *in vitro* phosphorylation of the truncations could be detected using Phos-tag™ gel electrophoresis technology. Overnight cultures of RN6734 bacterial strains were sonicated to lyse bacterial membranes, followed by centrifugation. Cell supernatant was then treated with Antarctic phosphatase to dephosphorylate proteins for use as controls in Phos-tag™ electrophoresis. Phosphorylated proteins were obtained solely by centrifugation of overnight cultures. Phosphorylated and dephosphorylated cell lysates were resuspended in sample buffer and electrophoresed on a 12% Phos-tag™ gel, followed by Western blot detection with an -His_6 antibody. A His_6 control of known molecular weight was run concomitantly, as migration in a Phos-tag™- gel is dependent on both size and phosphorylation status. As a result, pre-stained protein ladders often run poorly and provide an inadequate representation of molecular weight.

With the exception of the His_6 control in lane 11, all odd lanes represent phosphatase treated protein samples, as indicated by the singular band, seen in Figure 3.5. Even lanes contain untreated samples, which appear higher on the acrylamide gel than dephosphorylated samples, indicative of proteins in a phosphorylated state. The greater the number of phosphorylated residues within a protein sequence, the slower the protein migrates, due to interaction of phosphate groups with a divalent $MnCl_2$ present within the acrylamide gel.

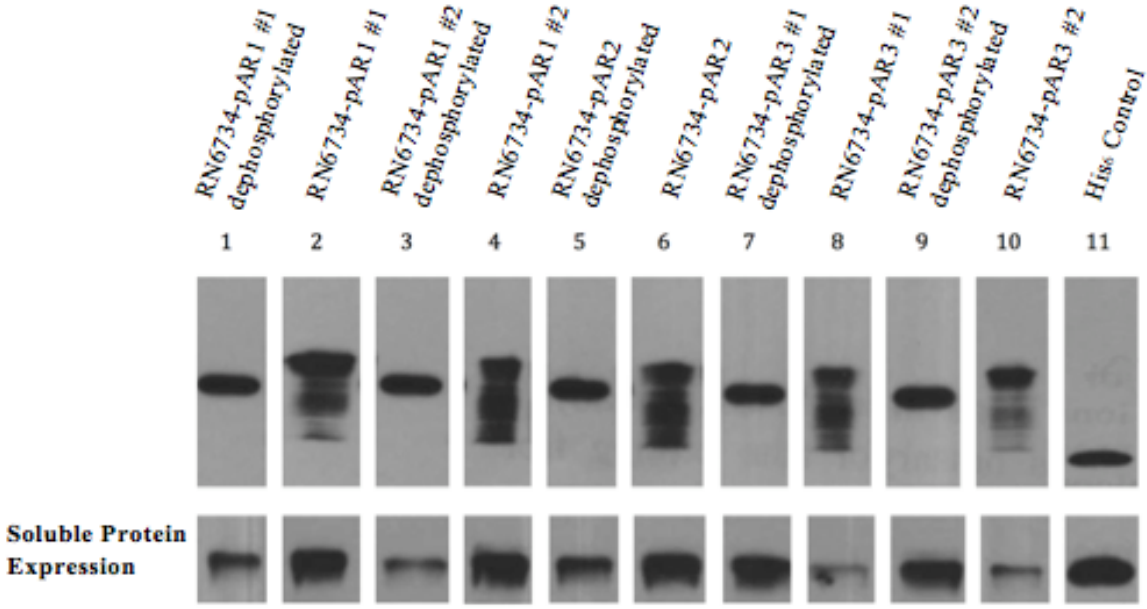

Figure 3.5: Phos-tag™ acrylamide gel analysis of AgrA truncations expressed in RN6734 indicates protein phosphorylation when compared to phosphatase treated controls. RN6734 cultures, expressing the AgrA truncation proteins, were resuspended and run on a 12% Phos-tag™ acrylamide gel. Parallel samples were treated with Antarctic phosphatase to remove any phosphate residues, as seen in odd numbered lanes. A His_6 control protein was run in conjunction to the test samples, as seen in lane 11. All RN6734 strains expressing the AgrA truncation proteins exhibit phosphorylation when compared to the phosphatase treated control, as indicated by the higher molecular weight banding.

3.4 qRT-PCR Analysis Suggests Only Minor Differences of RNAIII Expression in RN6734 versus RN6734 Truncations

Previous hemolysis assays suggests that AgrA truncations expressed in RN6734 strains act to inhibit the AgrC:AgrA interaction, resulting in a reduction of downstream hemolysis expression. RNAIII, the QS master regulator controlled by AgrA-induced P2 promoter activation, directly controls hemolysis production through RNA:RNA interactions that relieve secondary structures within the RNA sequence allowing for translation. To determine if the AgrA truncation construct inhibition of AgrC:AgrA resulted in a reduction of RNAIII production, thus mediating a downregulation of -hemolysin, qualitative real time PCR (qRT-PCR) was performed.

RNA was extracted from overnight cultures of *S. aureus* RN6734 strains as per manufacturer's instructions, followed by DNase treatment with DNase I to remove residual genomic DNA contamination. An aliquot of DNase treated RNA products were then subjected to reverse transcription by M-MLV reverse transcriptase to obtain cDNA. Two-step qRT-PCR using RNAIII-specific primers and probe sequences was performed to determine the number of RNAIII transcripts present in the RN6734 control strain versus AgrA truncation expressing strains. DNase non-RT samples were also subjected to qRT-PCR analysis to provide a control for the presence of background genomic DNA.

The visual graphical representation of the 40 cycle qRT-PCR reaction is displayed in Figure 3.6A. The greater the copies of a target gene that are present at the beginning of the assay, the fewer cycles of amplification are required to generate the number of amplicons that can be detected reliably. As such, cDNA treated samples that did not undergo RT, should only be present at later threshold cycle (Ct) numbers. Unfortunately,

numerous attempts at successfully eradicating genomic DNA have been largely unsuccessful, and non-RT samples subjected to only DNase treatment are still appearing at lower Ct values than RT-samples. In theory, RT-samples should then also be present are lower Ct values than indicated as RNAIII-specific primers would both amplify RT-produced cDNA and genomic RNAIII copies. This failure of genomic control, and high Ct value RT-samples suggests that the assay was not performed with any great success and continued troubleshooting is necessary. To confirm the graphical and numerical patterns seen through qRT-PCR analysis, samples were also run on a 1.5% agarose gel. Results from this confirm the patterns seen in Ct values, and the qRT-PCR graph.

Ct values were subsequently used to determine raw RQ values, indicating change in RNAIII transcript levels between the RN6734 control and RN6734 truncation expressing strains. RN6734-pAR1 variant 1 and RN6734-pAR3 variant 2 displayed the greatest reduction in RNAIII expression by 61.82-fold and 54.19-fold respectively. RN6734-pAR1 variant 2 and RN6734-pAR3 variant 1 exhibited relatively comparable reductions in RNAIII transcript production by19.43-fold and 19.29-fold respectively. While RN6734-pAR2 exhibited the lowest reduction in RNAIII transcript levels when compared to the RN6734 control at 4.2-fold. These results are inconsistent with inhibitor efficacies determined through *in vitro* hemolysis assays.

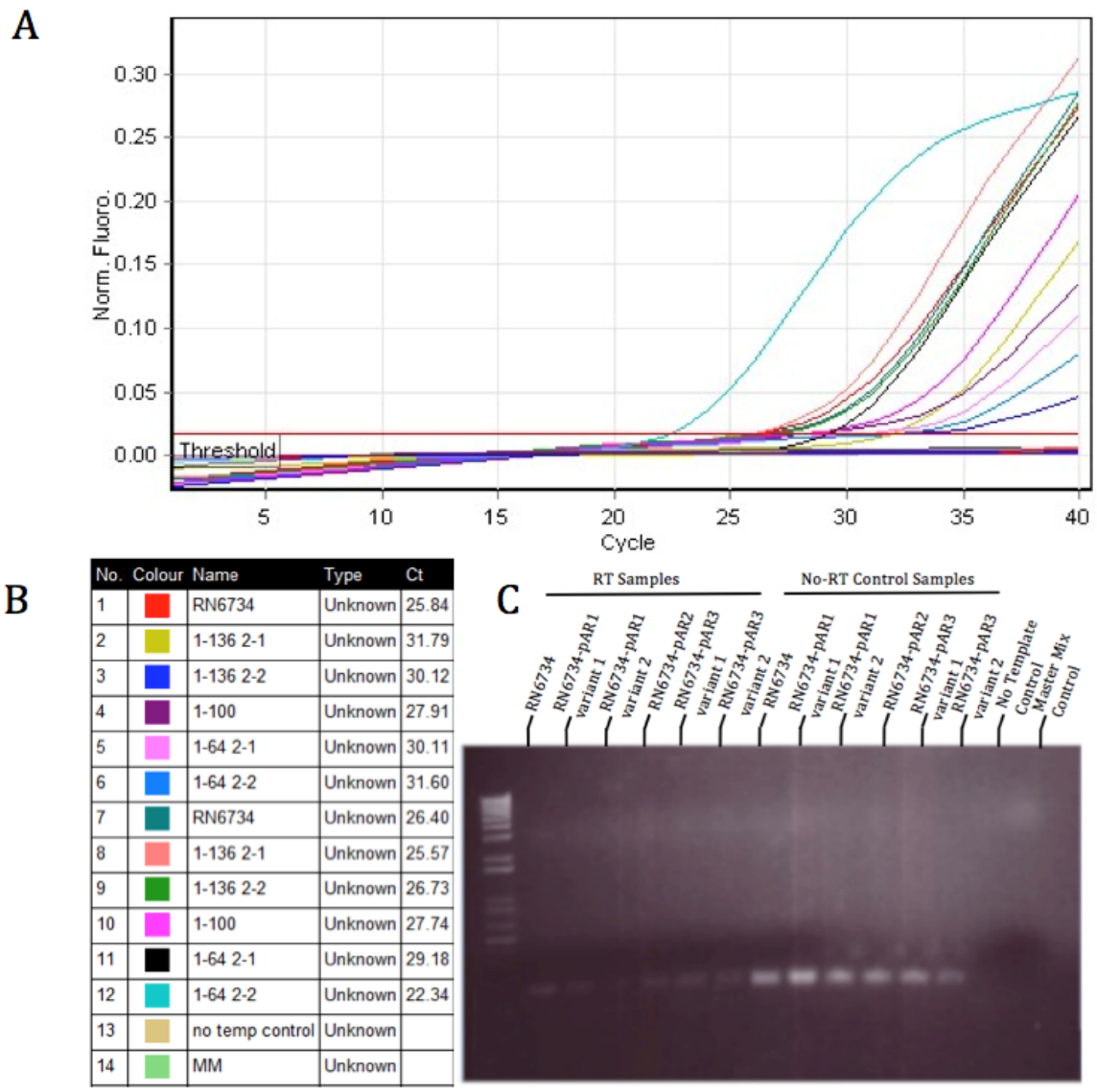

No.	Colour	Name	Type	Ct
1		RN6734	Unknown	25.84
2		1-136 2-1	Unknown	31.79
3		1-136 2-2	Unknown	30.12
4		1-100	Unknown	27.91
5		1-64 2-1	Unknown	30.11
6		1-64 2-2	Unknown	31.60
7		RN6734	Unknown	26.40
8		1-136 2-1	Unknown	25.57
9		1-136 2-2	Unknown	26.73
10		1-100	Unknown	27.74
11		1-64 2-1	Unknown	29.18
12		1-64 2-2	Unknown	22.34
13		no temp control	Unknown	
14		MM	Unknown	

Figure 3.6: qRT-PCR analysis suggests only minor differences of RNAIII transcript levels in RN6734 strains expressing AgrA truncation constructs versus the RN6734 control. RNA from both RN6734 (control) and RN6734 strains expressing truncation constructs was extracted. RNA levels were quantified, and 1 µg of each sample was treated with DNase, as per manufacturers instructions. An aliquot of DNase treated samples were subjected to M-MLV reverse transcription (RT). Both DNase treated samples and RT samples were subjected to qRT-PCR using RNAIII-specific primers and probe sequence. **A.** Graphical representation of the qRT-PCR reaction. **B.** The chart depicts the legend for the qRT-PCR graph, as well as Ct values for each sample. Samples 1-6 are RT-treated samples, while 7-12 are non-RT samples **C.** Samples subjected to qRT-PCR were run on a 1.5% agarose gel for visualization.

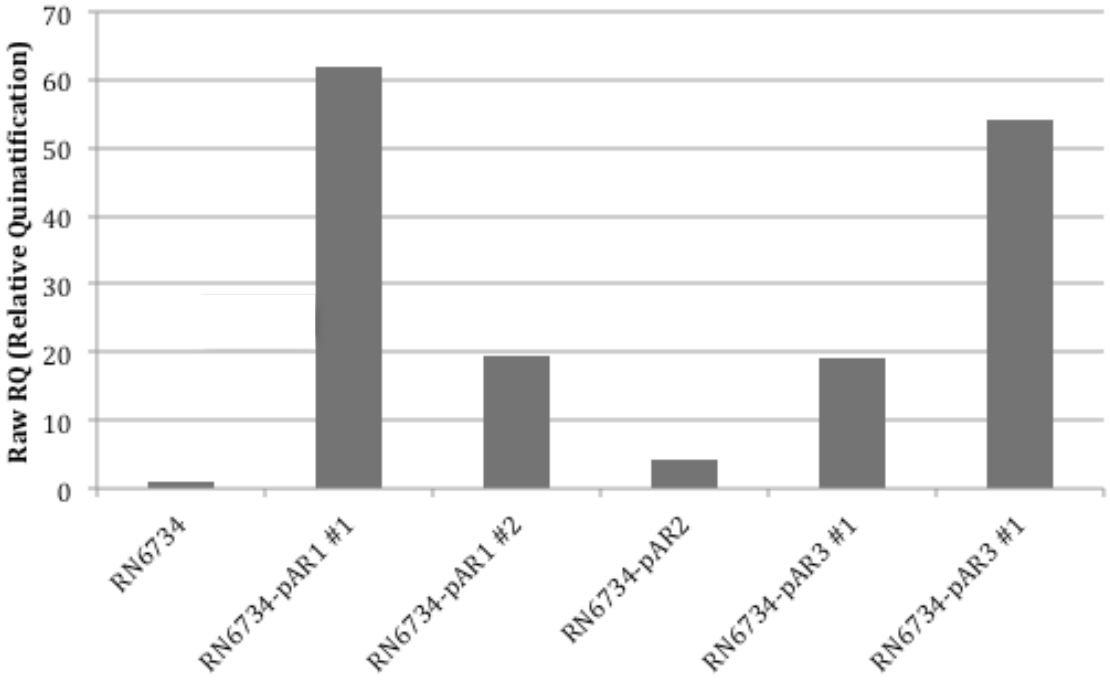

Figure 3.7 Relative quantification of RNAIII expression in RN6734 strains from qRT-PCR analysis. Ct values from qRT-PCR analysis were used to calculated relative expression of RNAIII in each RN6734 strain, relative to the RN6734 control. Raw relative quantity (RQ) of target was determined through the equation $RQ= 2^{-CT}$ where **Ct** is the difference between the control (RN6734) and test samples. By this calculation RN6734-pAR1 #1 and RN6734-pAR3 #2, $AgrA_{1-136}$ variant 1and $AgrA_{1-64}$ variant 2 respectively, display the greatest decrease in RNAIII transcript production. RN6734-pAR2, expressing $AgrA_{1-100}$ displays the least reduction in RNAIII expression by 4.2 fold.

3.5 A NLS-AgrA$_{1-64}$ Construct Does Not Facilitate Uptake into *S. aureus* Cells

Based on *in vitro* plate reader hemolysis assays, the AgrA truncation 1-64 performed the most adeptly as an inhibitor of quorum sensing and hemolysis production. Additionally, AgrA$_{1-64}$ is the smallest of the AgrA truncations and was resultantly tested for its ability to enter *S. aureus* RN6734 cells, an integral function for use of the truncations as putative peptide therapeutics. ArgA$_{1-64}$ was cloned with an N-terminal NLS sequence to promote cellular internalization, followed by a His-MBP sequence to aid in detection and protein solubility, to generate His-MBP-NLS-AgrA$_{1-64}$. An AgrA$_{1-64}$ construct lacking the NLS internalization sequence was also created to act as a negative control, generating His-MBP-AgrA$_{1-64}$. Overnight cultures of *S. aureus* RN6734 bacterial cultures were centrifuged and harvested cells were incubated with 100 μM of the His-MBP-NLS-AgrA$_{1-64}$ or His-MBP-AgrA$_{1-64}$ peptide solution. Cells were resuspended and incubated at 37ºC for 1 hour. Cells were harvested, washed with PBS, and loaded onto a SDS-PAGE gel for electrophoresis and -His Western blot analysis. Concomitantly, cell peptide resuspensions were incubated with proteinase K, a broad-spectrum serine protease, to digest any protein that may remain localized to the extracellular membrane. Proteinase K treated samples were run in parallel to native protein samples on the SDS-PAGE gel. If the NLS-peptide was effective in its ability to enter RN6734 cells, proteinase K treatment should have no effect and bands indicative of the protein construct should be present within the lysate samples of treated and untreated proteins.

Samples of RN6734 lysate, RN6734 supernatant and the input loading controls were run in parallel (Figure 3.8). The input loading controls were not treated with proteinase K, and merely demonstrate that both constructs are soluble and detectable on a

SDS-PAGE gel. RN6734 lysate samples for both the test and NLS-lacking control peptides treated with proteinase K demonstrate a complete absence of protein banding. Only lysate samples not treated with proteinase K demonstrate banding indicative of His-MBP-$AgrA_{1-64}$ and His-MBP-NLS-$AgrA_{1-64}$, as compared to the input controls. The banding pattern for the lysate samples mirrored that of the RN6734 supernatant samples; however, supernatant samples not treated with proteinase K displayed more prominent banding, indicative of a greater protein concentration.

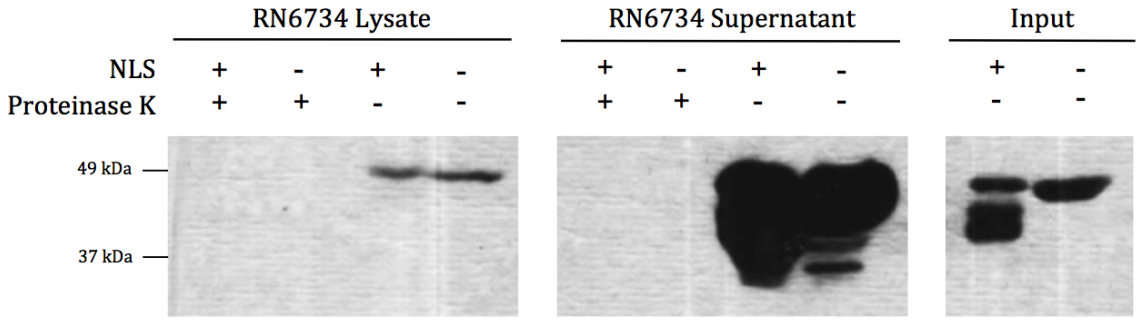

Figure 3.8: His-MBP-NLS-AgrA$_{1-64}$ is unable to enter *S. aureus* RN6734 cells. RN6734 cultures were harvested and incubated with 100 µM His-MBP-NLS-AgrA$_{1-64}$ peptide solution to allow peptide uptake. As a control, samples were concomitantly treated with 20 mg/mL proteinase K. Samples were run on a 12% SDS-PAGE gel and visualized by Western blot analysis with an -His antibody. NLS-AgrA$_{1-64}$ was unable to enter *S. aureus* RN6734 cells, and instead remained localized to the extracellular membrane as illustrated by the proteinase K controls.

CHAPTER FOUR

4.0 GENERAL DISCUSSION

4.1 AgrA Truncations Contain the Functional Domains Necessary to Inhibit AgrC:AgrA Interactions

The *agr* quorum sensing response regulator AgrA contains two fundamental domains; the N-terminal phosphorylation-activated switch REC domain and the C-terminal ~105-residue LytTR bacterial DNA-binding domain (Gao *et.al.*, 2009; Sidote *et.al.*, 2008). The crystal structure of the C-terminal DNA-binding domain of AgrA, represented by residues 137-238, bound to its DNA target was determined in 2008 by Sidote and colleagues, providing a general indication of the domain boundaries within the response regulator (Sidote *et.al.*, 2008). As such, the residues 1-136 could be hypothesized to contain the REC receiver domain responsible for the control of effector domain activity. The REC domain is ~120 residues, consistent with the N-terminal domain of AgrA, and mediates phosphoryl transfer and dephosphorylation events associated with response regulator control. Phosphorylation of the REC domain occurs at a conserved Asp residue, generating a high-energy acyl phosphate thereby providing the energy to drive conformational changes in the REC domain (Appendix 6.1.1)(Gao *et.al.*, 2009; West *et.al.*, 2001). Moreover, phosphorylation-induced dimerization or oligomerization is common among response regulator protein REC domains, often mediating the co-localization of DNA-binding domains and allowing for the interaction with direct-repeat sites comprising DNA recognition sequences (Gao *et.al.,* 2008).

As indicated by crystallization analysis of C-terminal LytTR DNA-binding domains, AgrA does dimerize with translation symmetry, mediated solely by the N-

terminal domains (Sidote *et.al.*, 2009). Furthermore, AgrA possess a hypothetical Asp phospho-acceptor residue at position 59, as well as two additional Asp/Glu residues within the active site that coordinate the essential Mg^{2+} and a conserved lysine that participates in the formation of a salt bridge with the phosphate ion (Gao *et.al.*, 2009). These patterns are consistent with those suggested by Basic Local Alignment Search Tool (BLAST) Conserved Domain analysis (National Centre for Biotechnology Information; Bethesda, MD, USA) (Figure 3.1) (Appendix 6.1.2).

AgrA truncations were designed with the maintenance of the conserved Asp phosphor-acceptor residue, as well as critical active site residues, in mind in order to facilitate the use of Phos-tag™ gel electrophoresis technology to analyze if truncated proteins were able to undergo HPK-mediated phosphorylation. The $AgrA_{1-136}$ truncation encompasses the entire REC domain, including critical active site residues, a dimerization domain at residues 110 and 111, and a hypothesized intermolecular recognition site comprising residues 62-67. In theory, this truncation should provide the best representation of the domain necessary to elicit AgrC:AgrA interaction, and thus should most effectively inhibit this process. The second truncation, $AgrA_{1-100}$ encompasses all but one active site residue, at position 107, and completely lacks the dimerization domain. As dimerization is phosphorylation-dependent the loss of the dimierization domain should not impede the funcationality of the recombinant protein as an inhibitor of AgrC:AgrA interaction. Loss of the active site residue at position 107 may however affect the efficiency of the phosphotransfer reaction, and thus alter the phosphorylation state of the truncation. Maintenance of the intermolecular recognition site should still promote

AgrC:$AgrA_{1-00}$ interaction, regardless of phosphorylation proficiency. Finally, $AgrA_{1-64}$ maintains only the phosphorylation site at Asp 59. The truncation directly severs the intermolecular recognition site, and obliterates all active site residues but those positioned N-terminally at residues 7 and residues 8. As such, it would be expected that $AgrA_{1-64}$ would represent the least effective inhibitor of AgrC:AgrA interaction, and thus demonstrate the lowest reduction in hemolytic capacity.

4.2 AgrA Truncations Inhibit Hemolysis in *S.* aureus RN6734

Quorum sensing in staphylococcal strains is largely responsible for two predominate phenotypic switches; the transcriptional downregulation of surface and cell wall-associated proteins employed during early pathogenesis and the postexponential-phase activiation of exproteins, including those of the hemolysin family (Queck *et.al.*, 2008; Novick *et.al.*, 2008). At the helm of this regulation lies the small RNA, RNAIII, which is localized divergently at the *agr* operon and is regulated directly by *agr*-mediated quorum sensing. RNAIII, termed a 'master regulator', facilitates the posttranscriptional regulation of virulence factors by RNA-RNA interaction and directly encodes *hld*, the delta hemolysin gene (Geisinger *et.al.*, 2012; Boisset *et.al.*, 2007). As a result, hemolysin production and subsequent hemolytic activity can be thought to be proportional to levels of quorum sensing activity, thus acting as a reporter of system function.

4.2.1 AgrA Truncations Inhibit RN6734 Hemolysis on Sheep's Blood Agar Plates

Sheep's blood agar (SBA) provides a qualitative method to observe differences in hemolysin production between wild-type *agr*$^{+}$ RN6734 strains, and those expressing the AgrA truncation constructs (Geisinger *et.al.*, 2012). RN6734, the negative control for AgrA truncation activity on AgrA:AgrC interaction, produces a strong -hemolysin and -hemolysin resulting in a predominate zone of clearing characteristic of this strain, as seen in Figure 3.2 (Ji *et.al.*, 2005). RN9688, an *agr*P_3-*lux* reporter where the P3-controlled RNAIII is replaced by the *lux* operon, acts as a positive control for truncation function as QS-inhibitors, as no hemolysis is observed (Wright *et.al.*, 2005). With the replacement of RNAIII, the RN6734 -hemolysin and RNAIII-encoded -hemolysin are not produced, thus no zone of clearing on SBA is feasible. The final control, the cloning intermediate RN4220, produces only -hemolysin resulting in a partially turbid zone of clearing. This strain acts as an indicator of residual RNAIII function; if the AgrC:AgrA interaction is only partially inhibited RNAIII should still be functional at basal or above-basal levels resulting in the production of -hemolysin (Wright *et.al.*, 2005; Ji *et.al.*, 2005). Consistent with previous strain-specific observations of SBA hemolysis, all controls produce the expected hemolytic patterns (Ji *et.al.*, 2005). None of the RN6734 strains transformed with pAR plasmids exhibit visible zones of hemolysis. While this indicates an inhibition of QS-mediated hemolysin production, basal levels of hemolysins may be still produced by truncation-expressing RN6734 strains and thus quantitative hemolysis analysis is a more accurate representation of the effect of AgrA truncations on quorum sensing inhibition.

4.2.2 AgrA Truncations Inhibit RN6734 Hemolysis in an *in vitro* Hemolysis Assay

AgrA, the response regulator of the *Staphylococcus aureus* quorum sensing system, contains two prototypical domains; the N-terminal REC domain which facilitates the catalysis of phosphoryl transfer from the AgrC HPK and the C-terminal effector domain responsible for eliciting the output of signal transduction, in the case of AgrA, DNA-binding and transcriptional up-regulation of P2- and P3-promoter controlled genes (Gao *et.al.*, 2009). As the N-terminal sequence of AgrA is predominately responsible for facilitating a transient interaction with AgrC, in addition to controlling the activity of the C-terminal effector domain, it was hypothesized that dominate negative decoys of the N-terminal region of AgrA would be sufficient to inhibit AgrC-mediated activation of AgrA, and the resulting downstream production of virulence factors, including the staphylococcal hemolysins. RN6734 strains transformed with plasmids expressing a series of AgrA truncations (denoted pAR1-3; Table 6.3.1, Appendix), were spotted onto SBA to provide preliminary indications of the effectiveness of these constructs as QS-inhibitors.

To further ascertain the efficacy of the AgrA truncation constructs to inhibit AgrC:AgrA interaction and hemolysin production in a quantitative manner, RN6734-pAR1-3 strains were subjected to an *in vitro* hemolysis plate assay. As a positive control, varying concentrations of the known QS-inhibitor AIPIII-D4A were tested concomitantly (Tal-Gan *et.al.*, 2013). AIPIII-D4A was the most effective inhibitor of RN6734 lysis at a 5 μM concentration, followed closely by RN6734-pAR3 strain variant 1 expressing the $AgrA_{1-64}$ truncation. Of the RN6734 transformation strains, those expressing the $AgrA_{1-64}$

truncations displayed the lowest percent lysis values, followed by the $AgrA_{1-100}$ truncation (RN6734-pAR2), and lastly the $AgrA_{1-136}$ constructs (RN6734-pAR1 variants 1 and 2).

These results are paradoxical to the hypothesized performance of the AgrA truncation constructs based on predicted domain architecture. It is possible, that the smaller size of the $AgrA_{1-64}$ truncation affords protection from proteolytic degradation, as compared to larger truncation constructs, thereby increasing the protein half-life and propensity toward disruption of the AgrC:AgrA interaction. Additionally, the smaller truncation constructs may be expressed more effectively, thus making them superior dominant negative decoys. HPK phospho-transfer to the REC Asp residue of AgrA is critical in facilitating the downstream conformational changes associated with effector domain activation and ensuing signal transduction (West *et.al.*, 2001). As such, the host of REC domain functional residues in the longer truncation constructs, specifically $AgrA_{1-136}$, may not be necessary in the blockade of AgrC:AgrA signal transduction. Phosphotransfer to the conserved Asp residue in the AgrA truncation proteins alone may be sufficient to inhibit AgrA activation.

4.2.3 AgrA Truncations Exhibit up to 94% Inhibition of RN6734 Hemolysis

To further emphasize the capacity of RN6734-expressed AgrA truncations to inhibit hemolysis values of percent lysis were converted to values of percent inhibition where untransformed RN6734 was employed as a negative control. Trends seen for percent lysis are inversely proportional to those for percent inhibition, as was expected. The known quorum sensing inhibitor, AIPIII-D4A, displayed the greatest inhibition of

hemolysis at 5 μM, followed closely by the RN6734-pAR3 strain variant 1 with approximately 94% inhibition. The capacity of AIP-III D4A to inhibit hemolytic activity of RN6734 decreased with a reduction in peptide concentration, and both of the strains expressing $AgrA_{1-136}$ (RN6734-pAR1 variants 1 and 2) performed less effectively as inhibitors of hemolysis production than the lowest concentration of AIPIII-D4A.

Regarded as the most potent *S. aureus* quorum sensing inhibitor to date, AIPIII-D4A at 5 μM is roughly comparable to the $AgrA_{1-64}$ truncation. However, AIPIII-D4A benefits as its activity as a dominant negative inhibitor is targeted extracellulary, competitively blocking the interaction of endogenous *S. aureus* AIPs with their cognate receptors. This property alone, in addition to previous evidence of efficacy in the nanomolar range, makes this peptide inhibitor more effective as a potential therapeutic (Tal-Gan *et.al.*, 2013). Efforts to internalize and optimize exogenously produced analogs of the AgrA truncation proteins would have to be undertaken to fully elucidate the possibility of these proteins acting as viable *S. aureus* therapeutics.

4.3 AgrA Truncation Constructs are Phosphorylated *in vitro*

Protein phosphorylation is integral for cell signaling, particularly with regards to two-component systems, and regulates most cellular processes including gene expression, cell division, metabolism, apoptosis, and differentiation (Tichy *et.al.*, 2011; Ptacek *et.al.*, 2006). Protein activity, localization, stability, and cellular interactions can all be controlled by phosphorylation. In the case of AgrA, and other response regulator proteins, phospho-transfer from the cognate HPK to a conserved aspartate phosphoacceptor, generates a high energy acyl phosphate that drives a conformational change in the

response regulator effector domain (Gao *et.al.*, 2006; West *et.al.*, 2001). Despite advances in phosphoproteomics, the study of phosphorylation events in response regulator proteins is largely complicated by a readily hydrolyzed phospo-Asp acylphosphate bond. Moreover, there are no antibodies currently available that recognize phospho-aspartate residues. In accordance with a recent publication from Barbieri and colleagues (2008), Phos-tag™ gel electrophoresis technology can effectively be employed to detect phosphorylation of aspartate residues in response regulator proteins.

As such, it was hypothesized that the RN6734-expressed AgrA truncation proteins, all containing the Asp59 major site of phosphorylation, would exhibit evidence of phosphorylation when electrophoresed on a Phos-tag™ acrylamide gel. Phosphorylation of the truncation constructs would indicate transient interaction with AgrC and subsequent phospho-transfer, characteristic of the AgrC:AgrA interaction, thereby strengthening the conjecture that the truncation proteins act as efficient dominant negative AgrA decoys. Cellular lysate from RN6734 strains expressing the AgrA recombinant truncation constructs were treated with a phosphatase to produce dephosphorylated controls, or electrophoresed without dephosphorylation to observe the predicted phosphorylation event. All protein constructs exhibited a reduction in acrylamide migration, when compared to the dephosphorylated controls, indicative of phosphorylated proteins. As mentioned previously, Phos-tag™ technology is based on the use of a dinuclear metal complex in the presence of a Mn^{2+} equivalent that binds specifically to phosphate residues, retarding the movement of phosphorylated proteins through the acrylamide matrix depending on the extent of phosphomonoester dianions

present (Barbieri *et.al.*, 2008; Kinoshita *et.al.*, 2006). As such, dephosphorylated proteins will migrate farther on an acrylamide gel then their phosphorylated counterparts, as is seen in Figure 3.5.

The less prominent bands visible in phosphorylated samples are likely byproducts of phospho-Asp hydrolysis (Thomas *et.al.*, 2013; Koshland, 1952; Barbieri *et.al.*, 2008). Alternatively, these bands could represent nonspecific phosphorylation of one or more of the His-residues present in the AgrA sequence. To confirm that Phos-tag analysis selectively identifies the phosphorylated form of AgrA and that AgrA is not phosphorylated at a site other than the predicted Asp59 site of phosphorylation, a mutant AgrA could be constructed in which the aspartate residue at position 59 is substituted by an alanine residue. As Asp59 is the predominant site of phosphorylation, particularly with regards to the truncation constructs, it is unlikely that other major sites of phosphorylation would be contributing to the phosphorylated state indicated by Phos-tag™ analysis. However, mutational studies would act as further confirmation of the importance of this site, and should result in the production of a construct that would exhibit no change in migration when compared to a dephosphorylated control.

4.4 Analysis Reveals Only a Minor Reduction in RNAIII Transcripts in RN6734 Strain Expressing AgrA Truncations

Qualitative fluorescence-based real-time PCR has become a critical tool for basic research, molecular biology, biochemistry, and biotechnology, and is the method of choice for the detection of low abundance mRNA (Bustin, 2000; Bustin, 2002). Numerous cellular decisions implicated in survival, growth, and differentiation are

reflected in patterns gene expression (Bustin, 2000). In *S. aureus* in particular, population based activation of quorum sensing signaling systems directly alters patterns of gene expression, facilitating a bacterial phenotypic switch (Novick *et.al.*, 2008). At the heart of this regulation lies the multifunctional messenger and antisense molecule RNAIII. The complex RNA, and 'master regulator' of *agr* QS, encodes δ-hemolysin (nucleotides 85-165) and controls its expression through regulation by the 3'end of the RNA. Additionally, RNAIII post-transcriptionally regulates *hla* (α-hemolysis) through RNA:RNA interactions that unmask the ribosome binding site (George *et.al.*, 2007; Novick *et.al.*, 2008). RNAIII is directly regulated by activated AgrA, through binding and expression from the P3 promoter. As such, RNAIII was identified as a viable target to analyze alterations in transcript levels and gene expression in the presence of the AgrA truncation constructs.

RNA extracted from RN6734 control or AgrA-expressing strains was subjected to DNase treatment followed by M-MLV reverse transcription to obtained cDNA. Both DNase treated non-RT samples and DNase treated RT samples were subjected to qRT-PCR using RNAIII specific primers and probe sequences. DNase treated non-RT samples were included as background controls for genomic DNA contamination. As mentioned previously, in theory these samples should appear in later cycles, with higher Ct numbers if minimal genomic DNA is present. Data from qRT-PCR analysis suggests that DNase non-RT samples appear at early Ct values, when compared to RT-treated samples. This is opposite of what would be expected in the absence of DNA contamination. Moreover, RT-treated samples should still appear prior to (lower Ct value) than DNase treated non-

RT samples, as RNAIII amplification could occur from both the genomic DNA contamination and RT-based cDNA. RNA samples were extracted using a RNA-specific column-based kit, versus a whole nucleic acid extraction, were treated with DNase I multiple times, and were subjected to RT using the Qiagen Quanitect Reverse Transcription kit which includes the gDNA enzyme for the elimination of genomic DNA. Even with these steps, genomic DNA is undoubtedly still present calling into question the validity of any results obtained from this assay. Unfortunately, research has also suggested that there continues to be significant contamination of RNA, on the scale of 50-80% of purified nucleic acid, highlighting one of the pitfalls of qRT-PCR technology (Bustin, 2002). Moreover, the efficiency of RNA to cDNA conversion is dependent on template abundance, and different priming approaches used to synthesis cDNA can have effect on RT success (Bustin *et.al.*, 2005). During the course of RT experiments performed in this study, random primers were used. This approach primes the reverse transcript at multiple points along each RNA template and the majority of cDNA synthesized in this manner is ribosomal RNA-derived. As a result, the mRNA target if produced in low levels may not be primed proportionally. To combat this in future experiments, target-specific primers should be used for RT, providing the most comprehensive and accurate generation of transcript-proportional cDNA (Bustin *et.al.*, 2005; Bustin *et.al.*, 2000).

If the presence of high genomic DNA contamination is to be ignored, then a measure of relative expression, or in this case reduction of expression as compared to RN6734, can be determined through the use of the equation $RQ=2^{-\Delta\Delta Ct}$, where $\Delta\Delta Ct$ is the

normalized change in Ct values between the control (RN6734) and test samples. In the case of qRT-PCR, and in ideal situations, Ct values should be normalized to an internal reference gene, such as a housekeeping gene, with stable and predictable mRNA expression. Despite numerous normalization strategies, this still remains the most perverse problem for quantification of qRT-PCR (Bustin *et.al.*, 2005). The highly conserved housekeeping gene β-actin is frequently used for normalization of qRT-PCR involving eukaryotic cells, but is not appropriate for use with bacterial *S. aureus* for obvious reasons (Condeelis *et.al*, 2005). As such future experiments should employ the staphylococcal gene *rho*, a transcriptional termination factor and housekeeping gene, for normalization, thus garnering a more all encompassing and accurate indication of changes in gene transcription in *S. aureus* strains expressing AgrA truncations (Theis *et.al.*, 2007).

Contrary to previous results from *in vitro* hemolysis assays, RN6734-pAR1 variant 1 and RN6734-pAR3 variant 2, expressing $AgrA_{1\text{-}136}$ and $AgrA_{1\text{-}64}$ respectively, displayed the greatest reduction in RNAIII transcript levels as compared to the RN6734 control. Surprisingly, RN6734-pAR3 variant 1 and RN6734-pAR1 variant 2 displayed almost comparable levels of transcript reduction by 19.29- and 19.43-fold respectively. These results, while likely skewed as a result of genomic DNA contamination, suggest that the $AgrA_{1\text{-}136}$ variant 1 truncation and $AgrA_{1\text{-}64}$ variant 2 truncation reduce RNAIII transcript production to the greatest extent, by 61.82- and 54.19-fold respectively. As per hemolysis assay data, RN6734-pAR3 variant 1 was expected to have the greatest impact on RNAIII expression, with RN6734-pAR3 variant 2 coming a close second, RN6734-pAR2 third, and RN6734-pAR1 variants 2 and 1 in fourth and fifth. It is possible that

transcripts within these two predominant samples were more stable for undefined reasons, RT-steps were more effective, or that background genomic DNA was present at a greater concentration. The latter is most likely, as these samples had the lowest Ct values, indicating the highest number of pre-existing transcripts at the start of the reaction.

Alternative targets for qRT-PCR should be considered, as RNAIII transcription may be upregulated even in the presence of low levels of activated AgrA. Moreover, RNAIII transcription is regulated by binding of the staphylococcal accessory regulator A (SarA), a winged helix transcription factor, to the P3 promoter. Only in the complete absence of AgrA is RNAIII expression halted (George *et.al.*, 2007). Additional steps to eliminate background genomic DNA, and the use of template-specific primers in RT steps may also aid in better elucidation of the effects of AgrA truncations on QS-mediated gene expression.

4.5 A NLS-AgrA$_{1-64}$ Construct Does Not Facilitate Uptake into *S. aureus* Cells

Effective uptake of peptide or small molecule therapeutic agents to block intracellular targets has proved a formidable challenge. The passive uptake of genes, polypeptides and small molecules into cells is prohibitive due to size constraints, and smaller oligonucleotides and peptides may be too hydrophobic to cross the cellular membrane (Dokka *et.al.*, 2000; Ragin *et.al.*, 2002). In eukaryotic cells, several approaches have been exploited to mediate import of DNA including viral vectors, cationic lipids and oligomers. These approaches have been drastically improved by the discovery that the human immunodeficiency virus (HIV)-1 Tat protein could efficiently

travel across cellular membranes in a receptor-independent fashion, leading to the determination of the minimal nuclear targeting region of this protein (Ragin *et.al.*, 2002). Similarly, discovery of the cationic peptide family of nuclear localization signal sequences has furthered the proficiency of cellular peptide uptake, specifically with regards to peptide and small molecule therapeutics whose molecular targets are localized to the nucleus (Ragin *et.al.*, 2002; Lange *et.al.*, 2007).

Though predominantly employed for cellular uptake into eukaryotic cells due to the presence of the characteristic NLS-importin pathway, we wanted to determine if addition of this sequence would aid in cellular uptake of small peptides into *S. aureus* Gram-positive cells. The $AgrA_{1-64}$ truncation was chosen for both its small size and previously determined efficacy as an inhibitor of QS-mediated hemolysis production. To generate control and test peptides a His-MBP sequence was cloned N-terminally to the $AgrA_{1-64}$ sequence followed by the prototypical NLS (YGRKKRRQRRR) in the test peptide only, generating His-MBP-NLS-$AgrA_{1-64}$ and His-MBP-$AgrA_{1-64}$. The *E. coli* MBP sequence, encoding the maltose binding protein, has been recognized as one of the most effective solubilizing agents, improving the yield, enhancing solubility, and promoting proper folding of its fusion partners (Raran-Kurussi *et.al.*, 2012; Sun *et.al.*, 2011). After incubation with either the test or control peptide, samples from both RN6734 lysate and RN6734 supernatant were obtained. Lysate samples should be indicative of protein constructs able to enter the cell, while protein detection in supernatant samples would indicate inability of cellular uptake. A subset of each sample were also treated with the protease proteinase K, to digest any extracellular proteins that were ineffective in cell entry, thus giving a clear indication of the success of NLS-mediated cellular uptake. Input

controls were run in parallel to confirm the presence and solubility of protein constructs. RN6734 lysate samples treated with proteinase K displayed no banding, while untreated samples indicated only faint banding suggesting a small proportion of both the test and control constructs localized to the extracellular membrane. The lack of banding in proteinase K treated samples suggests that regardless of the presence of the NLS signal, no protein was able to enter *S. aureus* RN6734 cells. The pattern of banding in lysate samples mirrored those of the supernatant, while one predominant exception; the banding for untreated test and control samples within the supernatant fraction displayed predominant, heavy bands suggesting that the highest concentration of peptide protein constructs is neither localized nor affixed to the extracellular membrane, but rather free-floating in solution. These results indicate that the neither the NLS nor NLS-lacking control protein construct is able to enter into *S. aureus* cells, likely due to the lack of NLS-associated machinery within the bacterial system.

The difficulty of entry of small peptide therapeutics into bacterial cells largely confounds the inhibition of intracellular targets. While $AgrA_{1-64}$ is a highly effective inhibitor when expressed from an intracellular exogenous plasmid, its ability to act as a potent therapeutic is dependent upon cellular uptake from an external peptide source. At 64 amino acids, and almost 200 nucleotides, simple diffusion across the bacterial membrane is likely not an option and further truncations of the sequence would need to be carried out to optimize peptide size and function. Regardless, diffusion proficiency is an uncontrollable variable and may depend upon membrane composition of *S. aureus*

subspecies; a designated cell penetrating peptide sequence or cellular uptake mechanism would be more effective in ensuring peptide entry and distribution.

4.6 Summary

4.6.1 AgrA Truncations as Inhibitors of Quorum Sensing

Truncations of the AgrA response regulator protein displayed competency as inhibitors of QS-mediated *S. aureus* hemolysis, specifically with regards to the $AgrA_{1-64}$ truncation. Though originally hypothesized to perform the least effectively due to the lack of numerous functional domain regions within the N-terminal AgrA REC domain that were previously thought to be necessary for AgrC:AgrA interaction, $AgrA_{1-64}$ diminished hemolysis production by approximately 94%, comparable with the most potent QS-inhibitor known to date. $AgrA_{1-100}$ displayed the second greatest inhibition of *S. aureus* hemolysis, followed lastly by the full-length AgrA N-terminal region, $AgrA_{1-136}$. These results suggest that the intermolecular recognition site, and a vast majority of the active site residues may not be necessary for the inhibition of AgrC:AgrA interactions. Rather, the $AgrA_{1-64}$ truncation may act as a dominant negative decoy for AgrC phospho-transfer to AgrA instead of direct binding. By blocking phosphorylation of AgrA, and consequently AgrA activation and dimerization, the 1-64 truncation effectively inhibits the AgrA:DNA interaction necessary for continuation of the QS-signal cascade and ultimate virulence factor production. As such, further optimization of the 1-64 truncation may be attempted by maintaining the Asp phospho-acceptor residue while further truncating the protein from the N-terminus. A smaller peptide may be more effectively

expressed and less likely to be degraded, whilst still maintaining its function of sequestering phosphate residues from AgrA.

4.6.2 Cellular Uptake of Truncation Peptides

Cellular uptake of $AgrA_{1-64}$ or other optimized peptides is essential for their use as eventual therapeutics. Intracellular targets have long posed problems with regards to cell entry and uptake, making extracellular receptor sites and protein targets preferred. Addition of a NLS sequence to the N-terminal of $AgrA_{1-64}$ did not mediate cellular uptake, and due to the size of the protein truncation, simple diffusion is likely not feasible. As such, optimization of the truncation should be considered to further reduce the peptide size and aid in cellular uptake. Moreover, alternative cell penetrating sequences may have to be considered to make $AgrA_{1-64}$ a viable therapeutic.

4.6.3 Limitations of this Study

Due to the poor expression of recombinant AgrA and AgrC proteins, alternative avenues to study the inhibition of their interaction needed to be considered and employed. Original experiments centered on the purification of recombinant AgrA and AgrC proteins, in addition to AgrA truncation proteins, for the use in protein pull down assays. It should be noted that full length AgrC is not soluble due to its function as a transmembrane sensor histidine kinase and as such only the C-terminal cytoplasmic domain could be cloned for expression. Additionally, though localized to the cytoplasm, full length AgrA is not soluble and thus only the N-terminal AgrC interacting domain was

considered. Posed with expression constrains, a staphylococcal expression vector for the expression of AgrA truncation proteins was then deemed the most viable method to observe potential inhibition of the AgrC:ArgrA interaction. Truncations were cloned into the expression vector, which was eventually transformed into RN6734 for observation of hemolysis production. While this avenue allows for a more accurate representation of QS-inhibition and AgrC:AgrA interactions, it is likely that intracellular expression of the truncation proteins results in a higher concentration of inhibitor present then would be seen from extracellular delivery.

4.7 Future Directions

As with any project, especially those in science, new discoveries and progress inevitably lead to more questions and research, such is the case here. Due to constraints in both time and resources, avenues of further research mentioned herein were not pursued, however they would provide new invaluable insights into the story of quorum sensing inhibition in *S. aureus*.

4.7.1 CopN Transformation Control to Determine Specificity of QS Inhibition by AgrA Truncations

In order to determine the specificity of AgrA truncation-mediated inhibition of the AgrC:AgrA interaction and thus downstream virulence production in the *agr* quorum sensing circuit, a non-native protein control known to have no effect on staphylococcal processes should be tested. CopN, the chlamydial outer protein N, is a type three secretion effector protein essential for chlamydial virulence, and has been studied

previously in our laboratory (Archuleta *et.al.*., 2011). No known orthologs to CopN exist in staphylococcal strains, suggesting that non-specific inhibition of *S. aureus* quorum sensing or other off-target effects on cellular processes are unlikely. Moreover, at approximately 50 kDA, CopN is relatively similar in size as AgrA. To determine if inhibition of quorum sensing by the AgrA truncations was specific, and not a direct result of extreme protein overexpression or disruption of cellular homeostasis, CopN or other analogous proteins should be cloned into the pCN47 staphylococcal shuttle vector, transformed into RN6734 and tested in parallel with the previously examined AgrA truncation constructs. The control protein should exhibit no appreciable reduction in the hemolytic capacity of RN6734 and no change in RNAIII transcript production in qRT-PCR analysis when compared to the RN6734 control.

4.7.2 Mutational Analysis of the Aspartate Phosphoacceptor in AgrA Truncations

As mentioned previously, Phos-tag™ acrylamide electrophoresis has brought about a new age in the analysis of phosphorylated proteins, specifically with regards to phospho-aspartate residues. Analysis of the phosphorylation states of the AgrA truncation proteins, when compared to dephosphorylated controls, indicate the presence of lower molecular weight bands inconsistent with phosphorylation of the predominant phospho-accepting residue. It is possible that these faster migrating bands are representative of the non-specific phosphorylation of histidine residues within the protein sequence. To confirm that the phospho-aspartate at residue 59 is the principal phosphorylation site Asp59 could be mutated to a non-phosphorylatable alanine residue and subjected to Phos-

tag™- analysis, as was performed by Barbieri and colleagues (2008). These mutational studies would serve to further highlight the importance of Asp59 as the phopho-acceptor, and aid in the explanation of the unexpected banding pattern seen in previous Phos-tag™ electrophoresis experiments.

4.8 Closing Remarks

Staphylococcus aureus has emerged as one of the most effective pathogens of our day and age through its rapid adaption to environmental niches, development of numerous antibiotic resistance phenotypes, and the immense societal and financial burden of staphylococcal infections. The two-component signal transduction system of *S. aureus* quorum sensing is integral to staphylococcal virulence and persistence of infection. As such, in a post-antibiotic era, novel therapeutics to this bacteria and this QS system are integral. Truncations of the response regulator protein AgrA have shown effective inhibition of QS-mediated hemolysis production, and have performed at levels comparable to the most potent inhibitor known to date. While these dominant negative decoys of AgrA phosphorylation are effective when expressed intracellulary, their efficacy as potential therapeutic inhibitors is limited by a lack of mechanisms for cellular uptake. Novel techniques, peptide optimization, and further experiments need to be performed in order validate the results demonstrated herein. Nonetheless, peptide-based inhibitors for two component systems, specifically *S. aureus* QS, is a feasible approach to block downstream signaling and virulence. This approach is also beneficial in terms of acquired resistance, as bacteria are unlikely to develop resistance to an amino acid

sequence that is integral to their cellular function and survival. *S. aureus* will continue to be a prominent area of research for vaccine development and peptide and small molecule therapeutics in an age where resistance to antimicrobial compounds in commonplace.

CHAPTER FIVE

5.0 REFERENCES

Adhikari RP, & Novick RP. (2008). Regulatory organization of the staphylococcus *sae* locus. *Microbiology*. 154: 949-959

Atkinson S, & Williams P. (2009). Quorum sensing and social networking in the microbial world. *J. R. Soc. Interface.* 6: 959-978

Barbieri CM, & Stock AM. (2008). Universally applicable methods for monitoring response regulator aspartate phosphorylation both in vitro and in vivo using Phos-tag-based reagents. *Anal. Biochem.* 376: 73-82

Bassler BL. (1999). How bacteria talk to each other: regulation of gene expression by quorum sensing. *Curr. Opin. Microbiol.* 2: 582-587

Bassler BL. (2002). Small Talk: Cell-to-Cell Communication in Bacteria. *Cell*. 109: 421-424

Benito Y, Kolb FA, Romby P, Lina G, Etienne J, & Vandenesch F. (2000). Probing the structure of RNAIII, the *Staphylococcus aureus agr* regulatory RNA, and identification of the RNA domain involved in repression of protein A expression. *RNA*. 6: 668-679

Benjamin HJ, Nikore V, & Takagishi J. (2007). Practical management: community-associated methicillin-resistant *Staphylococcus aureus* (CA-MRSA): the latest sports epidemic. *Clin. J. Sport. Med.* 17: 393-397

Boisset S, Geissmann T, Huntzinger E, Fechter P, Benridi N, Possedko M *et.al.* (2007). *Staphylococcus aureus* RNAIII coordinately represses the synthesis of virulence factors and the transcription regulator Rot by an antisense mechanism. *Genes & Dev.* 21: 1353-1366

Brink AJ. (2012). Does resistance in severe infections caused by methicillin-resistant *Staphylococcus aureus* give you the 'creeps'? *Curr. Opin. Crit. Care.* 18: 451-459

Bustin SA. (2000). Absolute quantification of mRNA using real-time reverse transcription polymerase chain reaction assays. *J. Mol. Endocrinol.* 25: 169-193

Bustin SA. (2002). Quantification of mRNA using real-time reverse transcription PCR (RT-PCR): trends and problems. *J. Mol. Endocrinol.* 29: 23-39

Bustin SA, Benes V, Nolan T, & Pfaffl MW. (2005). Quantitative real-time RT-PCR – a perspective. *J. Mol. Endocrinol.* 34: 597-601

Camilli A, & Bassler BL. (2006). Bacterial Small-Molecule Signaling Pathways. *Science*. 311: 1113-1116

Casino P, Rubio V, & Marina A. (2010). The mechanism of signal transduction by two-component systems. *Curr Opin Struct Biol*. 20: 763-771

Chambers HF, & DeLeo FR. (2009). Waves of Resistance: *Staphylococcus aureus* in the Antimicrobial Era. *Nat. Rev. Microbiol.* 7: 629-641

Charpentier E, Anton AI, Barry P, Alfonso B, Fang Y, & Novick RP. (2004). Novel cassette-based shuttle vector system for gram-positive bacteria. *Appl Environ Microbiol.* 70: 6067-6085

Chen L, Tsou L, & Chen F. (2009). Ligand-Receptor Recognition for Activation of Quorum Sensing in *Staphylococcus aureus*. *J. Microbiol.* 47: 572-581

Chua KYL, Howden BP, Jiang JH, Stinear T, & Peleg AY. (2013). Population genetics and the evolution of virulence in *Staphylococcus aureus*. *Infec. Gen. Evo.* In Press.

Condeelis J, & Singer RH. (2005). How and why does β-actin mRNA target? *Biol. Cell.* 97: 97-110

Deurenberg RH, & Stobberingh EE. (2008). The evolution of *Staphylococcus aureus*. *Infec. Gen. Evol.* 8: 747-763

Deurenberg RH, & Stobberingh EE. (2009). The molecular evolution of hospital- and community-associated methicillin-resistant *Staphylococcus aureus. Cuur. Mol. Med*. 9: 100-115

DiMondi VP. (2013). Review of Continuous-Infusion Vancomycin. *Ann. Pharmacother.* 47: 219-227g

Dokka S, & Rojanasakul Y. (2000). Novel non-endocytotic delivery of antisense oligonucleotides. *Adv. Drug. Deliv. Rev.* 44: 35-49

Dufour P, Jarraud S, Vandenesch F, Greenland T, Novick RP, Bes M *et.al.* (2002). High genetic variability of the *agr* lous in *Staphylococcus* species. *J. Bacteriol.* 184: 1180-1186

Dunman PM, Murphy E, Haney S, Palacios D, Tucker-Kellogg G, Wu S *et.al.* (2001). Transcription profiling-based identification of *Staphylococcus aureus* genes regulates by the agr and/or sarA Loci. *J. Bacteriol.* 183: 7341-7353

Enright MC, Robinson DA, Randle G, Fiel EJ, Grundmann H, & Spratt BG. (2002). The evolutionary history of methicillin-resistant *Staphylococcus aureus* (MRSA). *Proc. Natl. Acad. Sci*. 99: 7687-7692

Feil EJ, Cooper, JE, Grundmann H, Robinson DA, Enright MC, Berendt T *et.al.* (2003). How Clonal is *Staphylococcus aureus? J. Bacteriol.* 185: 3307-3316

Feng Y, Chen CJ, Su LH, Hu S, Yu J, & Chiu CH. (2008). Evolution and pathogenesis of *Staphylococcus aureus*: lessons learned from genotyping and comparative genomics. *FEMS Microbiol. Rev.* 32: 23-37

Gao R, & Stock AM. (2009). Biological Insights from Structures of Two-Component Proteins. *Annu. Rev. Microbiol*. 63: 133-154

Geisinger E, Adhikari R, Jin R, Ross H, Novick RP. (2006). Inhibition of rot translation by RNAIII, a key feature of *agr* function. *Mol. Microbiol.* 61: 1038-1048

Geisinger E, Chen J, & Novick RP. (2012). Allele-Dependent Differences in Quorum-Sensing Dynamics Result in Variant Expression of Virulence Genes in *Staphylococcus aureus*. *J. Bacteriol.* 194: 2854-2864

Geisinger E, George EA, Muir TW, & Novick RP. (2008). Identification of Ligand Specificity Determinants in AgrC, the *Staphylococcus aureus* Quorum-sensing Receptor. *J. Biol. Chem.* 283: 8930-8939

Geisinger E, Muir TW, & Novick RP. (2009). *agr* receptor mutants reveal distinct modes of inhibition by staphylococcal autoinducing peptides. *Proc. Natl. Acad. Sci*. 106: 1216-1221

George EA, Novick RP, & Muir TW. (2008). Cyclic Peptide Inhibitors of Staphylococcal Virulence Prepared by Fmoc-Based Thiolactone Peptide Synthesis. *J. Am. Chem. Soc.* 130: 4914-4924

Geogre EA, & Muir TW. (2007). Molecular Mechanisms of *agr* Quorum Sensing in Virulent Staphylococci. *Chem. Bio. Chem.* 8: 847-855

George Cisar EA, Geisinger E, Muir TW, & Novick RP. (2009). Symmetric signaling within asymmetric dimmers of *Staphylococcus aureus* receptor histidine kinase AgrC. *Mol. Microbiol.* 74: 44-57

Gill SR, Fouts DE, Archer GL, Mongodin EF, DeBoy RT, Ravel J *et.al.* (2005). Insights on Evolution of Virulence and Resistance from the Complete Genome Analysis

of an Early Methicillin-Resistant *Staphylococcocus aureus* Strain and a Biofilm-Producing Methicillin-Resistant *Staphylococcus epidermidis* Strain. *J. Bacteriol*. 187: 2426- 2438

Goldstein EJC. (2012). Challenges for a Universal *Staphylococcus aureus* Vaccine. *Clin. Infect. Dis.* 54: 1179-1186

González JE, & Keshavan ND. (2006). Messing with Bacterial Quorum Sensing. *Microbiol. & Mol. Biol. Rev.* 70: 859-875

Gordon RJ, & Lowy FD. (2008). Pathogenesis of Methicillin-Resistant *Staphylococcus aureus* Infection. *Clin. Infect. Dis.* 46: S350-S359

Götz F, Bannerman T, & Schleifer KH. (2006). The Genera *Staphylococcus* and *Macrococcus*. *Prokaryotes*. 4: 5-75

Grundmann H, Aires-de-Sousa M, Boyce J, & Tiemersa E. (2006). Emergence and resurgence of meticillin-resistant *Staphylococcus aureus* as a public health threat. *The Lancet*. 368: 874-885

Giuliani A, & Rinaldi A. (2011). Beyond natural antimicrobial peptides: multimeric peptides and other peptidomimetic approaches. *Cell. Mol. Life. Sci.* 6: 2255-2266

Harragy N, Kerdudou S, & Herrmann M. (2007). Quorum-sensing systems in staphylococci as therapeutic targets. *Anal. Bioanal. Chem*. 387: 437-444

Hawkey PM, & Jones AM. (2009). The changing epidemiology of resistance. *J. Antimicrob. Chemother.* 64: i3-i10

Hecker M, Bercher D, Fuchs S, & Engelmann S. (2010). A proteomic view of cell physiology anf virulence of *Staphylococcus aureus*. *Int. J. Med. Microbiol*. 300: 76-87

Ito T, Katayama Y, Asad, K, Mori N, Tsutsumimoto K, Tiensasitorn C. *et.al.* (2001). Structural comparison of three types of staphylococcal cassette chromosome *mec* integrated in the chromosome in methicillin-resistant *Staphylococcus aureus*. *Antimicrob. Agents. Chemother*. 46: 2155-216

Ji G, Beavis R, & Novick RP. (1997). Bacterial interference caused by autoinducing peptide variants. *Science*. 276: 2027-2030

Jarraud S, Mougel C, Thioulouse J, Lina G, Meugnier H, Forey F *et.al.* (2002). Relationships between *Staphylococcus aureus* Genetic Background, Virulence Factors, *agr* Groups (Alleles), and Human Disease. *Infect. Immun.* 70: 631-641

Kavanaugh JS, Thoendel M, & Horswill AR. (2007). A role for type I signal peptidase in *Staphylococcus aureus* quorum sensing. *Mol. Microbiol.* 65: 780-798

Kinoshita E, Kinoshita-Kikuta E, Takiyama K, & Koike T. (2006). Phosphate-binding tag, a new tool to visualize phosphorylated proteins. *Mol. Cell. Proteomics*. 5: 749-757

Kirchdoerfer RN, Garner AL, Flack CE, Mee JM, Horswill AR, Janda KD *et.al.* (2011). Structural Basis for Ligand Recognition and Discrimination of a Quorum-quenching Antibody. *J. Biol. Chem.* 286: 17351-17358

Kloos WE. (1980). Natural populations of the genus *Staphylococcus*. *Ann. Rev. Microbiol.* 34: 559-592

Koenig RL, Ray RL, Maleki SJ, Smeltzer MS, & Hurlburt BK. (2004). *Staphylococcus aureus* AgrA binding to the RNAIII-agr regulatory region. *J. Bacteriol.* 186: 7549-7555

Koshland DE. (1952). Effect of catalysts on the hydrolysis of acetyl phosphate. Nucleophilic displacement mechanisms in enzymic reactions. *J. Am. Chem. Soc.* 74: 2286-2296

Kreiswirth BN, Lofdahl S, Betely MJ, O'Reilly M, Schlievert PM, Bergdoll MS, & Novick RP. (1983). The toxic shock syndrome exotoxin structural gene is not detectably transmitted by a prophage. *Nature*. 305: 709-712

Kurlenda J, & Grinholc M. (2012). Alternative therapies in *Staphylococcus aureus* diseases. *Acta. Biochim. Pol.* 59: 171-184

Kuroda M, Ohta T, Uchiyama I, Baba T, Yuzawa H, Kobayashi I *et.al.* (2001). Whole genome sequencing of meticillin-resistant *Staphylococcus aureus*. *Lancet.* 357: 1225-1240

Lange A, Mills, RE, Lange CJ, Stewart M, Devine SE, & Corbett AH. (2007). Classical Nuclear Localization Signals: Definition, Function, and Interaction with Importin α. *J. Biol. Chem.* 282: 5101-5105

Lazdunski AM, Ventre I, & Sturgis JN. (2004). Regulatory circuits and communication in Gram-negative bacteria. *Nat. Rev. Microbiol.* 2: 581-592

Lee BY, Singh A, David MZ, Bartsch SM, Slayton RB, Huang SS *et.al.* (2013). The economic burden of community-associated methicillin-resistant *Staphylococcus aureus* (CA-MRSA). *Clin. Microbiol. Infect.* 19: 528-536

Li J, Wang W, Xu SX, Magarvey NA, & McCormick JK. (2011). *Lactobacillus reuteri*-produce cyclic dipeptides quench *agr*-mediated expression of toxic shock syndrome toxin-1 in staphylococci. *Proc. Natl. Acad. Sci.* 108: 3360-3365

Lindsay JA. (2010). Genomic variation and evolution of *Staphylococcus aureus*. *Int. J. Med. Microbiol.* 300: 98-103

Lindsay JA, & Holden MT. (2004). *Staphylococcus aureus*: superbug, super genome? *Trends Microbiol.* 12: 378-385

Liu GY. (2010). Molecular Pathogenesis of *Staphylococcus aureus* Infection. *Pediatr. Res.* 65: 71R-77R

Lowy FD. (1998). *Staphylococcus aureus* infections. *N. Engl. J. Med.* 339: 520-532

Lu, Y, Yang J, & Sega E. (2006). Issues related to targeted delivery of proteins and peptides. *AAPS. J.* 8: E466-478

Lyon GL, Mayville P, Muir TW, & Novick RP. (2000). Rational design of a global inhibitor of the virulence response in *Staphylococcus aureus*, based in part on localization of the site of inhibition to the receptor-histidine kinase, AgrC. *Proc. Natl. Acad. Sci*. 97: 13330-13335

Lyons GJ, Wright JS, Christopoulos A, Novick RP, & Muir TW. (2002). Reversible and specific extracellular antagonism of receptor-histidine kinase signaling. *J. Biol. Chem.* 277: 6247-6253

Mayville P, Ji G, Beavis R, Yang H, Goger, M, Novick RP, & Muir TW. (1999). Structure-activity analysis of synthetic autoinducing thiolactone peptides from *Staphylococcus aureus* responsible for virulence. *Proc. Natl. Acad. Sci*. 96: 1218-1223

Melter O, & Radojević B. (2010). Samll colony variants of *Staphylococcus aureus* – review. *Folia. Microbiol.* 55: 548-558

Miller MB, & Bassler BL. (2001). Quorum Sensing in Bacteria. *Annu. Rev. Microbiol.* 55: 165-199

Moellering RC Jr. (2008). Current treatment options for community-acquired methicillin-resistant *Staphylcoccocus aureus* infection. *Clin. Infect. Dis.* 46: 1032-1037

Moellering RC Jr. (2012). MRSA: the first half century. *J. Antimicrob. Chemother.* 67: 4-11

Ng WL, & Bassler BL. (2009). Bacterial Quorum-Sensing Network Architectures. *Annu. Rev. Genet.* 43: 197-222

Novick RP. (2003). Autoinduction and signal transduction in the regulation of staphylococcal virulence. *Mol. Microbiol.* 48: 1429-1449

Novick RP, & Geisinger E. (2008). Quorum sensing in staphylococci. *Annu. Rev. Genet.* 42: 541-564

Novick RP, Ross HF, Projan, SJ, Kornblum J, Kreiswrith B, & Moghazeh S. (1993). Synthesis of staphylococcal virulence factors is controlled by a regulatory RNA molecule. *EMBO J.* 12: 3967-3975

Otto M. (2012). MRSA virulence and spread. *Cell. Microbiol.* 14: 1513-1521

Oun S, Redder P, Didier JP, François P, Corvaglia AR, Buttazzoni E *et.al.* (2013). The CshA DEAD-box RNA helicase is important for quorum sensing control in *Staphylococcus aureus*. *RNA Biol.* 10: 157-165

Pan Y, Cheng JT, Hale J, Pan J, Hancock RE, & Straus SK. (2007). Characterization of the Structure and Membrane Interaction of the Antimicrobial Peptides Aurerin 2.2 and 2.3 from Australian Southern Bell Frogs. *Biophys. J.* 92: 2854-2864

Park J, Jagasia R, Kaufmann GF, Mathison JC, Ruiz DI, Moss JA *et.al.* (2007). Infection control by antibody disruption of bacterial quorum sensing signaling. *Chem Biol.* 14: 1119-1127

Perry J, Koteva K, & Wright G. (2011). Receptor domains of two-component signal transduction systems. *Mol. Biosyst.* 7: 1388-1398

Prax M, Lee CY, & Bertram R. (2013). An update on the molecular genetics toolbox for staphylococci. *Microbiol.* 159: 421-435

Ptacek J, & Snyder M. (2006). Charging it up: global analysis of protein phosphorylation. *Trends. Genet.* 22: 545-554

Qiu R, Pei W, Zhang L, Lin J, & Ji G. (2005). Identification of the Putative Staphylococcal ArgB Catalytic Residues Involving the Proteolytic Cleavage of AgrD to Generate Autoinducing Peptide. *J. Biol. Chem.* 280: 16695-16704

Ragin AD, Morgan RA, & Chmielewski J. (2002). Cellular Import Mediated by Nuclear Localization Signal Peptide Sequences. *Chem. Biol.* 9: 943-948

Raina S, De Vizio D, Odell M, Clements M, Vahulle S, & Keshavarz T. (2009). Microbial quorum sensing: a tool or a target for antiomicrobial therapy. *Biotechnol. Appl. Biochem*. 54: 65-84

Raran-Kurussi S, & Waugh DS. (2012). The ability to enhance the solubility of its fusion partners is an intrinsic property of maltose-binding protein but their folding is either spontaneous or chaperone mediated. *PLoS One.* 7: 1-10

Reading NC, & Sperandio V. (2006). Quorum sensing: the many languages of bacteria. *FEMS Microbiol. Lett.* 254:1-11

Rehm SJ. (2008). *Staphylococcus aureus*: The new adventures of a legendary pathogen. *Clev. Clin. J. Med.* 75: 177-192

Rothfork JM, Dessus-Babus S, Van Wamel WJ, Cheung AL, & Gresham HD. (2003). Fibrinogen depletion attenuates *Staphylococcus aureus* infection by preventing density-dependent virulence gene up-regulation. *J. Immunol*. 15: 5389-5395

Rutherford ST, & Bassler BL. (2012). Bacterial Quorum Sensing: Its Role in Virulence and Possibilities for Its Control. *Cold Spring Harb. Perspect. Med.* 2: 1-25

Sakoulas G, Gold HS, Cohen RA, Venkataraman L, Moellering RC, & Eliopoulos GM. (2006). Effects of prolonged vancomycin administration on methicillin-resistant *Staphylococcus aureus* (MRSA) in a patient with recurrent bacteraemia. *Antimicrob. Chemother*. 57: 699-704

Schaffer AC, & Lee JC. (2008). Vaccination and passive immunization against *Staphylococcus aureus*. *Int. J. Antimicrob. Agents.* 32: S71-S78

Segarra-Newnham M. (2012). Pharmacoptherapy for Methicillin-Resistant *Staphylococcus aureus* Nosocomial Pneumonia. *Ann. Pharmacother.* 46: 1678-1687

Shinefield HR. (2006). Use of a conjugate polysaccharide vaccine in the prevention of invasive staphylococcal disease: is an additional vaccine needed or possible? *Vaccine*. 24: S2-S9

Shinefield HR, & Ruff NL. (2009). Staphylococcal Infections: A Historical Perspective. *Infec. Dis. Clin. North. Am.* 23: 1-15

Sidote DJ, Barbieri CM, Wu T, & Stock AM. (2008). Structure of the *Staphylococcus aureus* AgrA LytTR Domain Bound to DNA Reveals a Beta Fold with an Unusual mode of Binding. *Structure*. 16: 727-735

Slonczewski JL, & Foster JW. (2009). Bacterial Diversity at a Glance. *Microbiology: An Evolving Science.* Ed. Michael Wright. New York: W.W. Norton & Company Inc. Print

Song Y, Tai JH, Bartsch SM, Zimmerman RK, Muder RR, & Lee BY. (2012). The potential economic value of a *Staphylococcus aureus* vaccine among hemodialysis patients. *Vaccine*. 30: 3675-3682

Sun P, Tropea JE, & Waugh DS. (2011). Enhancing the solubility of recombinant proteins in *Escherichia coli* by using hexahitidine-tagged maltose-binding protein as a fusion partner. *Methods Mol. Biol.* 705: 259-274

Taga ME, & Bassler BL. (2003). Chemical communication among bacteria. *Proc. Natl. Acad. Sci*. 100: 14519-14554

Takahashi T, Satoh I, & Kikuchi N. (1999). Phylogenetic relationships of 38 taxa of the genus *Staphylococcus* based on 16S rRNA gene sequence analysis. *Int. J. Sys. Bacteriol.* 48: 725-728

Tal-Gan Y, Stacy DM, Fiegen MK, Koenig DW, & Blackwell HE. (2013). Highly Potent Inhibitors of Quorum Sensing in *Staphylococcus aureus* Revealed Through a Systematic Study of the Group-III Autoinducing Peptide. *J. Am. Chem. Soc.* 135: 7869-7882

Theis T, Skurray RA, & Brown MH. (2007). Identification of a suitable internal controls to study expression of a *Staphylococcus aureus* multidrug resistance system by quantitative real-time PCR. *J. Microbiol. Meth.* 70: 355-362

Thoendel M, & Horswill AR. (2009). Identification of *Staphylococcus aureus* AgrD Residues Required for Autoinducing Peptide Biosynthesis. *J. Biol. Chem.* 284: 21828-21838

Thomas SA, Immormino RM, Bourret RB, & Silversmith RE. (2013). Nonconserved Active Site Residues Modulate CheY Autophosphorylation Kinetics and Phosphodonor Preference.

Thompson S, & Townsend R. (2011). Pharmacological agents for soft tissue and bone infected with MRSA: Which agent and for how long? *Injury.* 42: S7-S10

Tichy A, Salovska B, Rehulka P, Klimentova J, Stulik J, & Hernychova. (2011). Phosphoproteomics: Searching for a needle in a haystack. *J. Proteom.* 74: 2786-2797

Tristan A, Bes M, Meugnier H, Lina G, Bozdogan B, Courvalin P *et.al.* (2007). Global distribution of Panton-Valentine leukocidin-positive methicillin-resistant *Staphylococcus aureus*, 2006. *Emerg. Infect. Dis.* 13: 594-600

Turovskiy Y, Kashtanov D, Paskhover B, & Chikindas ML. (2007). Quorum sensing: fact, fiction, and everything in between. *Adv. Appl. Microbiol.* 62: 191-234

Vandenesch F, Naimi T, Enright MC, Lina G, Nimmo GR, Heffernan H, Liassine N, Bes M, Greenland T, Reverdy ME, & Etienne J. (2003). Community-acquired methicillin-resistant *Staphylococcus aureus* carrying Pnaton-Valentine leukocidin genes; worldwide emergence. *Emerg. Infect. Dis.* 9: 978-984

Waldron DE, & Lindsay JA. (2006). Sau1: a Novel Lineage-Specific Type I Restriction-Modification System That Blocks Horizontal Gene Transfer into *Staphylococcus aureus* and Between *S. aureus* Isolates of Different Lineages.

Waters CM, & Bassler BL. (2005). Quorum Sensing: Cell-to-Cell Communication in Bacteria. *Annu. Rev. Cell Dev. Biol.* 21: 319-346

Wenzel RP, & Perl TM. (1995). The significance of nasal carriage of *Staphylococcus aureus* and the incidence of postoperative wound infection. *J. Hosp. Infect.* 31: 13-24

West AH, & Stock AM. (2001). Histidine kinases and response regulator protein in two-component signaling systems. *Trends. Biochem. Sci.* 26: 369-376

Wright III JS, Lyon GJ, George EA, Muir TW, & Novick RP. (2004). Hydrophobic interactions drive ligand-receptor recognition for activation and inhibition of staphylococcal quorum sensing. *Proc. Natl. Acad. Sci*. 101: 16168-16173

Wright III JS, Traber KE, Corrigan K, Benson SA, Musser JM, & Novick RP. (2005). *agr* Radiation: an Early Event in the Evolution of Staphylococci. *J. Bacteriol.* 187: 5585-5594

Zhang RG, Pappas T, Brace JL, Miller PC, Oulmassov T, Molyneaux JM *et.al.* (2002). Structure of a bacterial quorum-sensing transcription factor complexed with pheromone and DNA. *Nature*. 417: 971-974

CHAPTER SIX

6.0 APPENDICES

6.1 Supplementary Figures

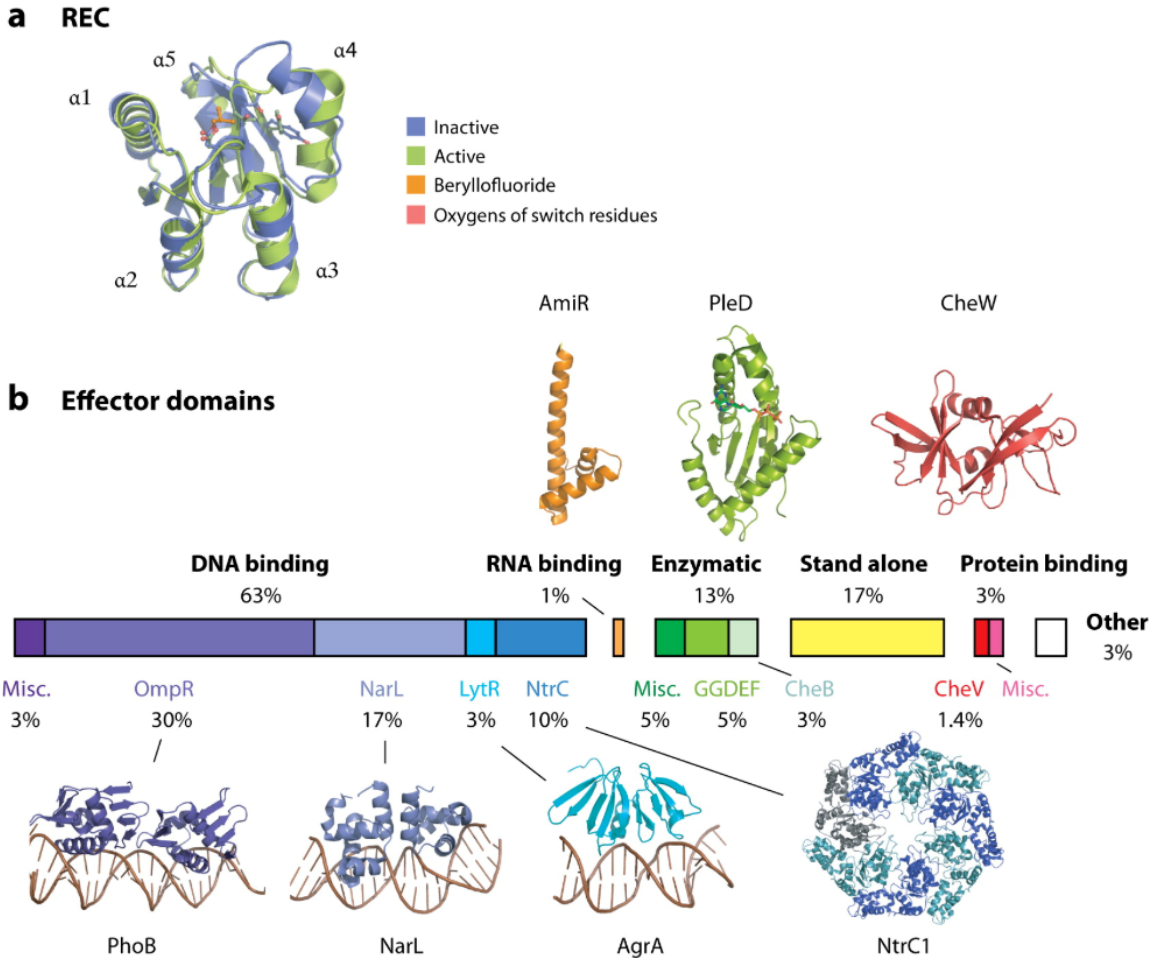

Figure 6.1.1: Structures of Response Regulator Domains (adapted from Gao *et.al.*, 2009). (*a*) The structure of active (green) and inactive (blue) REC receiver domains are shown. Beryllofluoride, used as a phosphoryl group mimic to stabilize the active conformation of the response regulator, is shown in orange. Active site residues are shown in ball-and-stick model. (*b*) The distribution of the diverse effector domains is shown by the horizontal bar, with response regulators grouped according to their functions. 3% of the DNA binding effector domain group is composed of LytTR-containing response regulators, including the *S. aureus* AgrA.

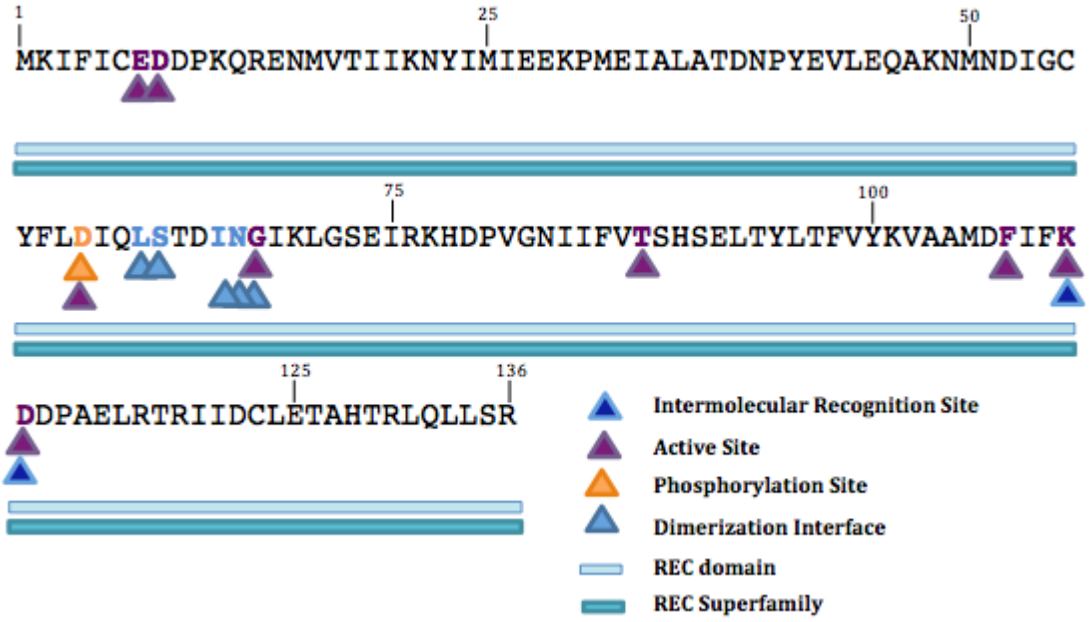

Figure 6.1.2: BLAST Conserved Domain Prediction for *S. aureus* AgrA N-terminal domain ($AgrA_{1-136}$). The N-terminal 1-136 amino acid sequence for AgrA was inputted into the National Centre for Biotechnology Information server BLAST to generate potential conserved domains. The REC superfamily and REC domain predictions are consistent with N-terminal domains of response regulator proteins. A phosphorylation site is indicated in orange, the active site residues are in purple, dimerization interface in blue, and intermolecular recognition site in indigo. These components are consistent with the conserved functions of the response regulator REC domain.

6.2 Oligonucleotide Primers

Table 6.2.1: Primer Sequences for PCR Amplification

Primer Name	Marker	Direction	Sequence
$AgrA_{1-136}F$	AgrA	F	GGCCTTGGATCCATG*CATCACCATCACC ATCAC*ATGAAAATTTTCATTTGCGAAGA
$AgrA_{1-136}R$	AgrA	R	GGCCTT**GAATTC**TCATTTAGACAACAA TTGTAAGC
$AgrA_{1-100}F$	AgrA	F	GGCCTTGGATCCATG*CATCACCATCACC ATCAC*ATGAAAATTTTCATTTGCGAAGA C
$AgrA_{1-100}R$	AgrA	R	GGCCTT**GAATTC**TTAGTAGACAAATGT TAAATAGGTAA
$ArgA_{1-64}R$	AgrA	R	GGCCTT**GAATTC**TTAAT=GTTGAAAGTT GAATATCTAAAA
CopNF	CopN	F	GGCCTTGGATCCATG*CATCACCATCACC ATCAC*ATGGATCAGTTAACAACGGATT
CopNR	CopN	R	GGCCTT**GAATTC**TTACCGGAAAATGGC GCGC
RNAIII	RNAIII	F	AGCCATCCCAACTTAATAACCA
RNAIII	RNAIII	R	TGTTTACGATAGCTTACATGCTAGA
RNAIII Probe	RNAIII	N/A	AGAGTTAGTTTCCTTGGACTCAGTGCT
NLS-F	NLS	F	GGGGACAAGTTTGTACAAAAAAGCAGG CTTAGATTACGATATCCCAACGACCGA AAACCTGTATTTTCAGGGCAGTTATGGC CGTAAAAAACG]
NLS-AgrAR	NLS/ AgrA	R	TCGCAAATGAAAATTTTCATACGACGT CGTTGACGGCGTTTTTTACGGCCATAAC T
NLS-AgrAF	NLS/ AgrA	F	AACGCCGTCAACGACGTCGTATGAAAA TTTTCATTTGCGAAGA
AgrAR	AgrA	R	GGGGACCACTTTGTACAAGAAAGCTGG GTCTTAAGTTGAAAGTTGAATATCTAA AAA‡

Bold nucleotides indicate the EcoRI restriction sequence; underlined sequences indicate the BamHI restriction sequence. Italicized nucleotides indicate a His_6 epitope tag.
] Primer contains the Gateway forward sequence; ‡ Primer contains the Gateway reverse sequence.

6.3 Bacterial Strains and Plasmids

Table 6.3.1: List of Bacterial Strains

Strain	Bacteria	Description	Source and/or Reference
RN4220	*S. aureus*	Non-lysogenic derivative of NCTC 8325 that accepts E. coli DNA; has agrA-8A mutation	R. Plaut / R.P. Adhikari (2008)
RN9688	*S. aureus*	*agr*-null derivative of RN6734 with pRN7141(pMK4*lux*; *agr*P3 drives *lux*) and pRN7130(*agr*P2 drives *agr*AC-I)	R.P. Novick/ J.S. Wright III (2005)
RN6734	*S. aureus*	Prototypical agr-I (derived from NCTC 8325), Φ13 lysogen	R.P. Novick (1993)
RN6734-pAR1	*S. aureus*	RN6734 transformed with plasmid pAR1	This study
RN6734-pAR2	*S. aureus*	RN6734 transformed with plasmid pAR2	This study
RN6734-pAR3	*S. aureus*	RN6734 transformed with plasmid pAR3	This study
XL-1	*E. coli*	F^- ompT gal dcm lon $hsdS_B(r_B^- m_B^-)$ λ(DE3 [lacI lacUV5-T7 gene 1 ind1 sam7 nin5])	Stratagene
BL21 (*DE3*)	*E. coli*	endA1 gyrA96(nal^R) thi-1 recA1 relA1 lac glnV44 F'[::Tn10 $proAB^+$ $lacI^q$ Δ(lacZ)M15] hsdR17($r_K^- m_K^+$)	Stratagene

Table 6.3.2: List of Plasmids

Plasmid	Description	Source and/or Reference
pCN47	pT181 based shuttle vector with an Erm cassette	P. Linder/ E. Charpentier (2004)
pAR1	pCN47 with *agrA*$_{1-136}$ inserted into the EcoRI and BamHI sites of the pUC19 MCS	This study
pAR2	pCN47 with *agrA*$_{1-100}$ inserted into the the EcoRI and BamHI sites of the pUC19 MCS	This study
pAR3	pCN47 with *agrA*$_{1-64}$ inserted into the the EcoRI and BamHI sites of the pUC19 MCS	This study
pDONR$_{201}$	*E. coli* Gateway® vector for the incorporation of *attL* sites, Kan^R	Invitrogen
pDEST$_{17}$	*E. coli* Gateway® expression vector for purification of proteins with N-terminal His$_6$-tag	Invitrogen
pHisMBP-*agrA*$_{1-64}$	*E. coli* Gateway® expression vector containing *agrA*$_{1-64}$ cloned into the *attL* and *attR* sites of the pHisMBP expression vector. Proteins contain a N-terminal His$_6$-MBP tag	This study